

POLITECNICO DI MILANO

School of Industrial and Information Engineering

Master of Science in Biomedical Engineering



POLITECNICO
MILANO 1863

**RECAPITULATING MONOCYTE EXTRAVASATION IN A
MICROFLUIDIC ORGANOTYPIC MODEL OF THE
OSTEOARTHRITIC JOINT**

Supervisor: Prof. Marco Rasponi

Co-supervisor: Dr. Silvia Lopa

Dr. Silvia Palombella

Eng. Matteo Moretti

Master Thesis by:

Federico Pigoli

Student ID:

883078

Academic year 2019-2020

Acknowledgements

I would first like to thank *Prof. Marco Rasponi* for the chance to join his microfluidics group at the Microfluidics and Biomimetic Microsystems Laboratory (MiMiC Lab) of Politecnico di Milano and for his availability during this work.

I also would like to thank *Eng. Matteo Moretti* for the opportunity to work with his group at the Cell and Tissue Engineering Laboratory (CTEL) at IRCCS Galeazzi Orthopedic Institute of Milan.

My sincere thank to *Dr. Silvia Lopa* for the recommendations during these months, for being always available and for her help.

A big thank to *Dr. Silvia Palombella* for her teachings, for her time and for being always available

A special thank to my family that made it possible, encouraging me every day to never give up and to continue my studies.

My greatest thank to Camilla for her love, her support and for always being there for me.

Table of contents

Acknowledgements.....	1
Table of contents	2
List of figures.....	4
Abstract.....	7
Sommario.....	14
1. Introduction	22
1.1. Osteoarthritis	22
1.1.1. General description	22
1.1.2. Synovial joint	22
1.1.3. OA as a whole-joint disease.....	23
1.1.4. Inflammation	25
1.1.5. Involved tissues.....	28
1.1.5.1. Articular cartilage	28
1.1.5.2. Synovial membrane	29
1.1.5.3. Synovial fluid	30
1.2. Microfluidics.....	30
1.2.1. General principals.....	30
1.2.2. Manufacturing of microfluidic devices	33
1.2.3. Microfluidics in biological applications	36
1.2.4. Models of OA.....	38
1.2.5. Extravasation models	39
2. Aim of the thesis.....	42
3. Materials and Methods	44
3.1. Fabrication of the microfluidic device	44
3.2. Biological Validation	47
3.2.1. Cell isolation and culture	47
3.2.1.1. Synovial fibroblast isolation.....	47
3.2.1.2. Articular chondrocyte isolation	48
3.2.1.3. Thawing of SFb and ACh and culture	49

3.2.1.4. Endothelial cells.....	49
3.2.1.5. Monocytes.....	49
3.2.2. Synovial Fluid.....	51
3.2.3. Cell embedding in fibrin hydrogel.....	51
3.2.4. Endothelial monolayer formation.....	51
3.2.5. Endothelial cell pre-conditioning.....	52
3.2.6. Model validation.....	53
3.2.7. Monocyte extravasation assay	53
3.2.8. Monocyte extravasation quantification.....	54
3.2.9. Statistical analysis.....	55
3.3. Cytotoxicity assay	56
3.3.1. Experimental design and procedure.....	56
4. Results	58
4.1. Biological validation.....	58
4.1.1. Description of the microfluidic device	58
4.1.2. Expression of adhesion molecules.....	59
4.1.3. Model validation.....	61
4.1.4. Monocyte extravasation assay	63
4.2. Cytotoxicity assay	65
5. Discussion.....	67
6. Conclusion and future perspectives	72
7. Bibliography	73

List of figures

Figure 1 – Internal structure of a synovial joint. (source: www.pdhpe.net).....	23
Figure 2 - Structural difference between healthy (left) and OA joint (right) [source https://www.creative-biolabs.com].....	24
Figure 3 – Representation of the extravasation process, showing in each phase the adhesion molecules involved. In response to a diverse range of proinflammatory triggers, that can stimulate leukocytes and vascular cells to initiate a cascade of leukocyte adhesion and motility responses. This enables optimal scanning of the vascular lumen for exit signals. Leukocyte rolling, firm attachment, and intravascular crawling are sequentially mediated by the indicated endothelial cell adhesion molecules and leukocyte endothelial selectin and integrin ligands, responses that are prerequisites to leukocyte migration through venular walls. A delicate balance between integrin-ligand microclusters allows arrested leukocytes to scan the endothelial lumen for chemotactic exit signals under hydrodynamic forces.	27
Figure 4 – Schematic representation of articular cartilage, showing all the zones that constitute it. From top to bottom it is possible to distinguish the superficial, middle and deep zone. [source: https://www.semanticscholar.org].	29
Figure 5 – Laminar streams of solutions of dye (in water) flowing in microfluidic channels. The fluid is flowing from the six channels on the left into the central channel on the right where flow is laminar [32].....	32
Figure 6 - Basic monomeric unit of polydimethylsiloxane [source: www.elflow.com]. .	34
Figure 7 - Schematic representation of the soft lithographic procedure for the realization of PDMS microfluidic devices	36
Figure 8 - Examples of organ-on-a-chip.....	38
Figure 9 - Cross-sectional image of Han’s microfluidic device in which are comprised: a medium channel on the left; an endothelial channel in the middle surrounded by two channels that include ECM components; a channel that comprise chemokine on the right [51].....	40
Figure 10 – Schematic representation of the microfluidic device developed by Bersini and Jeon, including an external 3D view (a), a 2D to view (b), and a 2D front view showing the transmigration step (c) [55].....	41
Figure 11 - Overview of the microfluidic device developed by Molteni et al. a) 3D representation of the device; b) schematic representation of the components present in the device; c) experimental set-up [53].	41

Figure 12 – Schematic representation of the device used in this project comprising all cell types used. From top to bottom: synovial membrane formed by synovial fibroblasts embedding a post-capillary venule formed by endothelial cells; synovial fluid channel resembling the joint cavity; articular cartilage formed by articular chondrocytes.	43
Figure 13 - (A) CAD representation of the microfluidic device for monocyte extravasation model; (B) Pillar specification, all dimensions are expressed in μm ; Cross-sectional representation of the device, all dimensions are expressed in μm	45
Figure 14 - Schematic representation of PDMS pouring, polymerization and detachment from the silicon wafer master	46
Figure 15 - Picture of the microfluidic device developed for this thesis. Channels for SFB seeding are evidenced in red, channel for ACh seeding is shown in green. All inlet accesses are obtained with 1 mm diameter puncher. Outlet accesses of gel compartments are obtained with 1 mm diameter puncher, outlet accesses of endothelial and synovial fluid channel are obtained with 4 mm diameter puncher.	47
Figure 16 - PBMCs isolation by density gradient centrifugation using Ficoll-Paque. After centrifugation PBMC were stratified between upper plasma layer and lower Ficoll layer while red blood cells were stratified at the bottom of the falcon tube.....	50
Figure 17 – Picture showing all types of cells used in our microfluidic chip. From top to bottom, in red synovial fibroblasts, in green HUVECs, in magenta monocytes and in green chondrocytes.	58
Figure 18 - Pictures showing immuno-detection of ICAM-1 (first row) and VCAM-1 (second row) on HUVECs subjected to perfusion at different flow rates (5 $\mu\text{L}/\text{h}$, 10 $\mu\text{L}/\text{h}$, 15 $\mu\text{L}/\text{h}$, 30 $\mu\text{L}/\text{h}$) or maintained in static condition. Specific signal of adhesion proteins is represented in magenta, HUVEC-GFP in green and nuclei in blue. Pictures representing VCAM-1 are presented without the green signal of the endothelial cells, since it would hide the magenta signal specific of the antibody.	59
Figure 19 - Pictures showing the expression of ICAM-1 and VCAM-1 in endothelial cells subjected to TNF- α alone or combined with perfusion at 30 $\mu\text{L}/\text{h}$. Specific signal of adhesion proteins is represented in magenta, HUVEC-GFP in green and nuclei in blue. Pictures representing VCAM-1 are presented without the green signal of the endothelial cells, since it would hide the magenta signal specific of the antibody.	60
Figure 20 - A) 3D reconstruction of confocal pictures showing monocyte extravasation in response to control medium (upper row) or chemokine mix (lower row). Extravasation was evaluated in chip pre-conditioned with perfusion at 30 $\mu\text{L}/\text{h}$ combined with TNF- α (right column) and compared to a control group maintained in static (left column); B) Quantification of data obtained from picture analysis with our automated macro to count	

the number of extravasated monocytes in the upper and lower compartment in all tested conditions.	62
Figure 21 - A) Pictures showing monocyte extravasation in response to synovial fluid from OA patients under static conditions (left column) or after perfusion with flow rate of 30 $\mu\text{L}/\text{h}$ combined with TNF- α (right column) compared to control group without synovial fluid. Extravasation was performed in complete system or in devices without supporting cells. Black pictures highlight the presence or not of supporting cells (SFb are shown in red in the synovial compartment and ACh in green in the cartilage compartment). Grey reconstructions highlight extravasated monocytes in magenta. B) Quantification of specifically extravasated monocytes (lower compartment) and non-specific extravasated monocytes (upper compartment) in all tested conditions.	64
Figure 22 - HUVEC viability in response to chemokine receptor antagonists suspended in RPMI (A) or in RPMI + EGM-2 (B) at two different concentrations compared to the control group without antagonists (red dashed line).	Errore. Il segnalibro non è definito.
Figure 23 - Quantification of HUVECs viability in response to chemokine receptors' antagonists suspended in RPMI or in RPMI + EGM-2 at two different concentrations after endothelial cells have been preconditioned with TNF- α compared to the control group without antagonists but equally treated with TNF- α (red dashed line).	66

Abstract

Introduction

Osteoarthritis (OA) is a degenerative joint disease and the most common form of arthritis. It is characterized by joint pain during movements, stiffness, loss of flexibility and swelling, and it is one of the most debilitating disease [1]. For a long time, OA has been considered as a simple wear and tear disease involving mainly the degeneration of the cartilage, with a collateral impact on the surrounding tissues. However, recent studies suggested to consider OA as a whole-joint disease, since all joint tissues contribute to disease progression [2]. Even though the sequential events leading to OA pathogenesis are still unknown, the inflammation of the synovial tissue is considered as one of the major components that drive the progression of this disease [3]. Inflammation involves the microvasculature of the synovial membrane and is characterized by an abnormal monocyte extravasation from post-capillary venules into the surrounding tissue. Extravasation is a highly regulated process that actively

involves both leukocytes and endothelial cells and is mediated by adhesion molecules, such as ICAM-1 and VCAM-1 [4].

Monocyte extravasation involves a series of sequential steps, which are tethering, rolling, adhesion and trans-endothelial migration (TEM). Once monocytes extravasate, they migrate through the extracellular matrix (ECM) towards a concentration gradient of inflammatory molecules accumulated in the synovial tissue [5]. After synovial membrane invasion, monocytes differentiate in macrophages and produce pro-inflammatory cytokines, such as Tumor Necrosis Factor- α (TNF- α) and Interleukin-1 β (IL-1 β). These pro-inflammatory cytokines act on chondrocytes by stimulating the production of matrix metalloproteinases (MMP) and inhibiting the synthesis of new ECM, finally leading to the cartilage destruction. Moreover, cytokines stimulate synovial fibroblasts to produce chemokines involved in the recruitment of monocytes, further contributing to

monocyte accumulation in the synovial tissue and thus causing a chronic inflammation [3].

Treatments able to inhibit joint deterioration in OA patients are currently missing and available drugs are directed only to alleviate pain and symptoms without counteracting OA progression. To fill this gap, in the recent years, novel chemical agents have been developed. Disease-modifying osteoarthritis drugs (DMOADs) aim to decrease cartilage degradation and inflammatory cytokine release, thus inhibiting OA progression and improving tissue function [6]. However, clinical trials testing anti-cytokine drugs so far showed no significant efficacy [7]. In this scenario, drugs targeting chemokine signaling involved in the recruitment of monocytes may represent a novel strategy to prevent the accumulation of these immune cells in synovial membrane, thus limiting the progression of inflammation during OA. As a first step towards the development of effective therapeutic strategies, a deep knowledge of the pathogenic mechanisms and of the involved factors is essential. In order to have an insight in the basic process of OA inflammation, it is

necessary to understand and dissect the process of monocyte extravasation towards the synovial membrane. Several *in vitro* models have been developed to study cell migration and extravasation, including the Boyden chamber. However, these models have major limitations, such as the gravity influence on cell migration, which does not allow understanding which factors impacted more on the extravasation, and the inability to perform the assay under conditions of physiological fluid flow and shear stress, which are fundamental for the expression of adhesion molecules involved in the extravasation process [8]. Microfluidics has recently emerged in biological research presenting many advantages compared to traditional systems, such as the reduction of sample volumes, precise temporal and spatial control of the biochemical environment, and the possibility to co-culture different types of cells in the same device, allowing to mimic tissues or organs in a single device, and producing the so called organs-on-chips [9].

Considering all these advantages, in this project we used a microfluidic device to mimic monocytes extravasation in the OA

joint. The device is a multi-channel chip that resembles the synovial membrane with a post-capillary venule, the articular cartilage and the joint cavity filled with synovial fluid. In particular, we used synovial fibroblasts (SFb) and articular chondrocytes (ACh) embedded in a fibrin hydrogel to resemble synovial membrane and articular cartilage, respectively, and endothelial cells to mimic a post-capillary venule (Fig. 1).

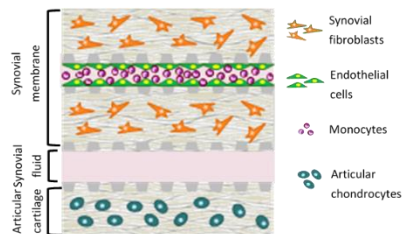


Fig. 1 - Schematic representation of the device used in this project comprising all cell types used.

In order to select the best pre-conditioning treatment, we firstly verified the expression of adhesion molecules directly involved in the extravasation process. In particular, we analyzed the expression of ICAM-1 and VCAM-1 in endothelial cells maintained in static conditions or subjected to different shear stress and in response to an inflammation stimulus. Then, we validated the model by assessing monocyte extravasation in response to a chemokine mix or to control medium. Afterwards, we evaluated the

chemoattractant effect of OA synovial fluid on monocyte extravasation. Moreover, we examined whether the presence of tissue-specific cells (SFb and ACh) could influence monocyte extravasation, comparing the extravasation in the complete system and in the system without tissue-specific cells. Considering monocyte extravasation as a possible target for future therapies, we hypothesize to use the same microfluidic model to study the effect of antagonists for chemokine receptors on monocytes. Since endothelial cells are sensible to culture conditions, the last part of the thesis was focused on a preliminary investigation on the cytotoxicity of antagonists for CCR1, CCR2, CCR3, CCR4, CCR5, and Cencriviroc (CVC), a molecule targeting both CCR2 and CCR5.

Material and methods

To perform the experiments of this project, synovial fibroblasts (SFb) and articular chondrocytes (ACh), were obtained from OA patients, embedded in fibrin hydrogels and injected in the respective channels in the microfluidic device. To simulate a synovial post-capillary venule, we used Human

Umbilical Vein Endothelial Cells-Green Fluorescent Protein (HUVEC-GFP) to generate an endothelial monolayer on the walls of the channel included in the synovial membrane compartment. In order to mimic the physiological conditions and the inflammation state occurring *in vivo*, HUVECs seeded in the device were subjected to a pre-conditioning treatment. To select the optimal parameters, we performed immunofluorescent assays to detect ICAM-1 and VCAM-1 expression in endothelial cells maintained in static or exposed to different flow rates (5 $\mu\text{L/h}$, 10 $\mu\text{L/h}$, 15 $\mu\text{L/h}$ and 30 $\mu\text{L/h}$) combined or not with TNF- α .

Once established the best pre-conditioning parameters, we validated the developed model quantifying the extravasation of primary human monocytes in response to a known chemokine mix composed of MIP-1 α , MCP-1, RANTES and MIP-1 β . After preconditioning the endothelial monolayer, monocytes isolated from human blood samples of healthy donors and stained with Vybrant™ cell-labeling solution DiD, were injected in the endothelialized channel and their

extravasation was detected. Afterwards, extravasation experiments were conducted to investigate the chemoattractant effect of synovial fluid on monocyte extravasation and whether the presence of tissue-specific cells (SFb and ACh) could influence this process. Therefore, we prepared chips injected with empty or cell-laden hydrogels. To visualize cells during the assay, we stained SFb and ACh with Vybrant™ Dil and Vybrant™ DiO cell-labeling solution, respectively.

The last part of the thesis was focused on the analysis of the cytotoxicity exerted on HUVECs by the antagonists for CCR1, CCR2, CCR3, CCR4, CCR5. In addition, we also evaluated the cytotoxicity of CVC, which inhibits both CCR2 and CCR5, and of all the antagonists combined together (excluding CVC). In these experiments, HUVECs were cultured in standard multi-well using the same culture protocols applied in the microfluidic chip. To evaluate whether antagonist toxicity could have a synergic effect with TNF- α , we established treatment with antagonists alone or after TNF- α exposure.

Results and discussion

The results of the immunofluorescence assay showed that the expression of ICAM-1 was stimulated as the shear stress increased compared to the static control. Conversely, endothelial cells in static condition did not express this adhesion molecule. On the other hand, VCAM-1 was expressed at very low levels and appeared to decrease with increasing the flow rate compared to static control. To test the influence of pro-inflammatory stimulation, we assessed the expression of ICAM-1 and VCAM-1 in endothelial cells maintained in static or subjected to flow rate at 30 $\mu\text{L/h}$, both in the presence and in the absence of TNF- α . The results evidenced that the expression of these adhesion molecules was upregulated upon TNF- α exposure compared to the condition without TNF- α . In particular, TNF- α stimulated the expression of ICAM-1 more in dynamic (30 $\mu\text{L/h}$) than in static condition, suggesting a synergic effect of flow and TNF- α . On the other hand, VCAM-1 was upregulated in the presence of TNF- α more in static condition than in samples subjected to dynamic condition,

confirming the trend observed with fluid flow only. Given these results, we selected the dynamic condition that induced the highest expression of the two adhesion molecules. Therefore, for the subsequent experiments, the endothelial monolayer was pre-conditioned with fluid flow at 30 $\mu\text{L/h}$ and TNF- α (Fig. 2).

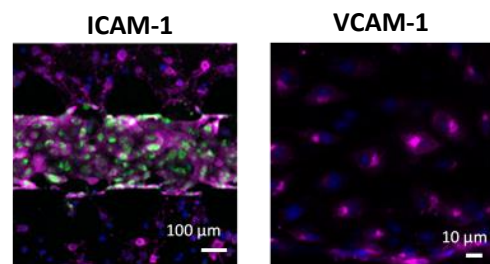


Fig. 2 - Pictures showing the expression of ICAM-1 and VCAM-1 in endothelial cells subjected to TNF- α with perfusion at 30 $\mu\text{L/h}$

The model validation experiments showed that the extravasation of monocytes was directional toward the chemokine channel, confirming that the observed extravasation was specific and driven by chemokine signaling. As we expected, monocyte extravasation in the presence of control medium was almost absent. Conversely, a high number of monocytes extravasated in response to the chemokine mix. Moreover, we verified that after endothelial pre-conditioning the number of extravasated cells was higher than in static chips, suggesting that the pre-conditioning

simulated better the *in vivo* conditions (Fig.3).

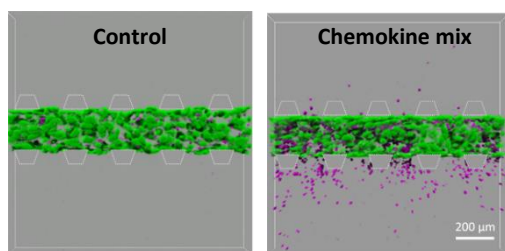


Fig. 3 - 3D reconstruction of confocal pictures showing monocyte extravasation in response to control medium or to a chemokine mix after pre-conditioning with 30 $\mu\text{L/h}$ fluid flow combined with $\text{TNF-}\alpha$

Subsequent extravasation assays showed that monocytes extravasated in the presence of OA synovial fluid, while in the presence of control medium they remained confined inside the endothelial channel, thus demonstrating the chemoattractant effect of OA synovial fluid. The directional extravasation towards the lower compartment induced by synovial fluid was significantly higher compared to the non-specific extravasation towards the upper compartment in all the tested conditions (Fig.4).

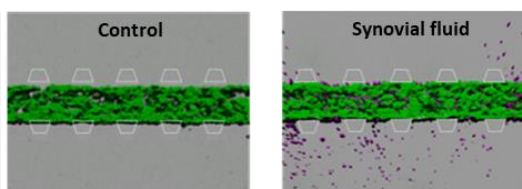


Fig. 4 - 3D reconstruction of confocal pictures showing monocyte extravasation in response to control medium or to synovial fluid after pre-conditioning with 30 $\mu\text{L/h}$ fluid flow combined with $\text{TNF-}\alpha$

Surprisingly, a higher number of monocytes extravasated in the system

without supporting cells (SFb and ACh) compared to the extravasation observed in the complete system. These results indicated that SFb and ACh do play a role in the extravasation process, making the complete system more similar to the *in vivo* condition than a simplified system.

Concerning the results of cytotoxicity assays, it emerged that all the antagonists had some cytotoxic effect on HUVECs, which decreased at low antagonist concentrations. Unexpectedly, all the antagonists combined together had a lower cytotoxic effect compared to the single antagonists. Also CVC cytotoxicity appeared to be lower than that of single antagonists, making it a promising antagonist to be tested in our device. HUVECs treated also with $\text{TNF-}\alpha$ showed overall a lower cytotoxicity in response to single or combined antagonists compared to HUVECs not exposed to $\text{TNF-}\alpha$. These preliminary data will be used in future to optimize the experimental conditions to test the antagonist and evaluate their ability to inhibit monocyte extravasation in our microfluidic model.

Conclusions and future perspectives

In this thesis, we validated a microfluidic organotypic device that models the process of monocyte extravasation to the osteoarthritic joint. We optimized the pre-conditioning parameters and assessed monocyte extravasation in response to a mix of known chemoattractant molecules or to patient-derived synovial fluids. In the next future, the results obtained in the cytotoxicity assay will be applied to use the chip as a platform to screen anti-chemokine drugs.

Sommarario

Introduzione

L'osteoartrosi (OA) è una malattia articolare degenerativa ed è la forma più comune di artrosi. Questa patologia provoca dolori articolari durante i movimenti, rigidità, perdita di flessibilità e gonfiore ed è una delle malattie più debilitanti [1]. Per molto tempo l'OA è stata considerata una semplice malattia da usura, che coinvolgeva principalmente la degenerazione della cartilagine con un impatto collaterale sui tessuti circostanti. Tuttavia, recenti studi hanno suggerito di considerare l'OA come una malattia dell'intera articolazione poiché tutti i tessuti articolari contribuiscono alla progressione della malattia [2]. Anche se gli eventi sequenziali che portano alla patogenesi dell'OA sono ancora sconosciuti, l'infiammazione del tessuto sinoviale è considerata uno dei principali componenti che guidano la progressione di questa malattia [3]. L'infiammazione coinvolge la microvascolatura della membrana sinoviale ed è caratterizzata da un livello anomalo dell'extravasazione dei monociti dalle venule post-capillari verso i tessuti circostanti. L'extravasazione è un processo altamente

regolato che coinvolge attivamente sia i leucociti che le cellule endoteliali ed è mediata dalle molecole di adesione, come ICAM-1 e VCAM-1 [4].

L'extravasazione dei monociti comporta una serie di passaggi sequenziali, che sono "*tethering*", rotolamento, adesione e migrazione transendoteliale. Una volta extravasati, i monociti migrano attraverso la matrice extracellulare (ECM) verso un gradiente di concentrazione di molecole chemoattraenti accumulate nel tessuto sinoviale [5]. Dopo l'invasione della membrana sinoviale, i monociti differenziano in macrofagi e producono diverse citochine pro-infiammatorie, come il fattore di necrosi tumorale- α (TNF- α) e l'interleuchina-1 β (IL-1 β). Queste citochine pro-infiammatorie agiscono sui condrociti stimolando la produzione di metallo-proteinasi della matrice (MMP) e inibendo la sintesi di nuova ECM, portando, infine, alla distruzione della cartilagine. Le citochine, inoltre, stimolano i fibroblasti sinoviali a produrre chemochine coinvolte nel reclutamento dei monociti, contribuendo ulteriormente all'accumulo di monociti nel tessuto sinoviale, causando quindi un'infiammazione cronica [3].

Attualmente mancano trattamenti in grado di inibire il deterioramento dell'articolazione nei pazienti con OA e i farmaci disponibili sono diretti solo ad alleviare il dolore e i sintomi senza contrastare la progressione dell'OA. Per colmare questa lacuna, negli ultimi anni sono stati sviluppati nuovi agenti chimici. I "*Disease-modifying osteoarthritis drugs*" (DMOAD) mirano a ridurre la degradazione della cartilagine e il rilascio di citochine infiammatorie, inibendo così la progressione dell'OA e migliorando la funzione dei tessuti [6]. Tuttavia, gli studi clinici che hanno testato i farmaci anti-citochine non hanno mostrato un'efficienza significativa finora [7]. In questo scenario, farmaci che interagiscono con le chemochine coinvolte nel reclutamento dei monociti, possono rappresentare una nuova strategia per prevenire per l'accumulo di queste cellule immunitarie nella membrana sinoviale, limitando così la progressione dell'infiammazione durante l'OA.

Il primo passo essenziale verso lo sviluppo di strategie terapeutiche efficaci è una profonda conoscenza dei meccanismi patogenetici e dei fattori coinvolti. Al fine

di avere una visione del processo alla base dell'infiammazione durante l'OA, è necessario comprendere e analizzare il processo di extravasazione dei monociti verso la membrana sinoviale. Diversi modelli *in vitro* sono stati sviluppati per studiare la migrazione e l'extravasazione delle cellule, come la camera di Boyden. Tuttavia, questi modelli presentano grandi limitazioni come, per esempio, l'influenza della gravità sulla migrazione delle cellule, che non permette di capire quali fattori abbiano avuto un impatto maggiore sull'extravasazione, e l'impossibilità di effettuare saggi in condizioni fisiologiche di flusso e forze di taglio, fondamentali per l'espressione delle molecole di adesione coinvolte nel processo di extravasazione [8].

La microfluidica è recentemente emersa nella ricerca biologica presentando numerosi vantaggi rispetto ai sistemi tradizionali, come la riduzione dei volumi dei campioni, un preciso controllo temporale e spaziale dell'ambiente biochimico e la possibilità di co-coltivare diversi tipi di cellule nello stesso dispositivo, permettendo di simulare tessuti o organi in un unico dispositivo,

producendo i cosiddetti “*organ-on-chip*” [9].

Considerando tutti questi vantaggi, in questo progetto abbiamo utilizzato un dispositivo microfluidico in grado di simulare l’extravasazione dei monociti in un’articolazione affetta da OA. Il dispositivo è un chip multicanale che imita la membrana sinoviale con una venula post-capillare, la cartilagine articolare e la cavità articolare riempita con liquido sinoviale. In particolare, abbiamo usato fibroblasti sinoviali (SFb) e condrociti articolari (ACh) incorporati in gel di fibrina per mimare rispettivamente la membrana sinoviale e la cartilagine articolare, e le cellule endoteliali per mimare una venula post-capillare. Per selezionare il miglior pre-trattamento, abbiamo prima verificato l’espressione di molecole di adesione direttamente coinvolte nel processo di extravasazione. In particolare, abbiamo analizzato l’espressione di ICAM-1 e VCAM-1 nelle cellule endoteliali mantenute in condizioni statiche o soggette a differenti sforzi di taglio e in risposta a uno stimolo infiammatorio. Successivamente abbiamo validato il modello valutando l’extravasazione dei monociti in risposta a

una mix di chemochine o a un terreno di controllo. Dopodiché, abbiamo valutato l’effetto chemoattraente del liquido sinoviale derivato da pazienti con OA sull’extravasazione dei monociti. Inoltre, abbiamo valutato se la presenza delle cellule tessuto-specifiche (SFb e ACh) possa influenzare l’extravasazione dei monociti, confrontando l’extravasazione nel sistema completo e nel sistema senza cellule tessuto-specifiche.

Considerando l’extravasazione dei monociti come possibile obiettivo per future terapie, ipotizziamo di utilizzare lo stesso modello microfluidico per studiare l’effetto degli antagonisti dei recettori delle chemochine sui monociti. Poiché le cellule endoteliali sono sensibili alle condizioni di coltura, l’ultima parte della tesi si è focalizzata sull’indagine preliminare della citotossicità degli antagonisti per CCR1, CCR2, CCR3, CCR4, CCR5 and Cencriviroc (CVC), una molecola che interagisce sia con CCR2 e con CCR5.

Materiali e metodi

Per eseguire gli esperimenti di questo progetto, fibroblasti sinoviali (SFb) e condrociti articolari (ACh), sono stati ottenuti da pazienti affetti da OA,

incorporati in gel di fibrina e iniettati nei rispettivi canali nel dispositivo microfluidico. Per simulare una vena post-capillare sinoviale, abbiamo utilizzato “Human Umbilical Vein Endothelial cells-Green Fluorescent Protein” (HUVEC-GFP) per generare un monostrato di endotelio sulle pareti del canale incluso nel compartimento della membrana sinoviale (Fig. 1).

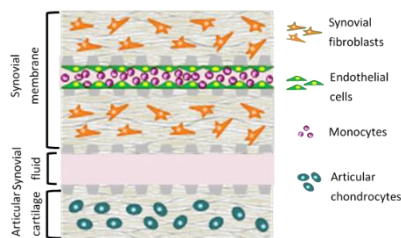


Fig. 1 - Rappresentazione schematica del dispositivo utilizzato in questo progetto comprendente tutti i tipi di cellule utilizzate.

Al fine di imitare le condizioni fisiologiche e lo stato di infiammazione che si verificano *in vivo*, le HUVEC seminate nel dispositivo sono state sottoposte a un trattamento di pre-condizionamento. Per selezionare i parametri ottimali abbiamo eseguito saggi di immunofluorescenza per individuare l'espressione di ICAM-1 e VCAM-1 nelle cellule endoteliali mantenute in statico o sottoposte a diverse portate (5 $\mu\text{L/h}$, 10 $\mu\text{L/h}$, 15 $\mu\text{L/h}$ and 30 $\mu\text{L/h}$) combinate o meno con TNF- α .

Una volta stabiliti i migliori parametri di pre-condizionamento, abbiamo validato il modello sviluppato, quantificando l'extravasazione di monociti umani primari in risposta a un mix di chemochine noto composto da MIP-1 α , MCP-1, RANTES e MIP-1 β . Dopo aver pre-condizionato il monostrato endoteliale, i monociti, isolati da campioni di sangue umano di donatori sani e colorati con Vybrant™ cell-labeling solution DiD, sono stati iniettati nel canale endotelializzato e la loro extravasazione è stata rilevata. Successivamente, sono stati condotti esperimenti di extravasazione per studiare l'effetto chemoattraente del liquido sinoviale sull'extravasazione dei monociti e se la presenza delle cellule tessuto-specifiche (SFb e ACh) possa influenzare questo processo. Pertanto, abbiamo preparato chip iniettati con gel vuoti o carichi di cellule. Per visualizzare le cellule durante il test, abbiamo colorato SFb e ACh con Vybrant™ DiI and Vybrant™ DiO cell-labeling solution, rispettivamente.

L'ultima parte della tesi è stata focalizzata sull'analisi della citotossicità esercitata sulle HUVEC dagli antagonisti per CCR1, CCR2, CCR3, CCR4, CCR5. Inoltre,

abbiamo valutato anche la citotossicità di CVC, che inibisce sia CCR2 che CCR5, e di tutti gli antagonisti combinati tra loro (escluso CVC). In questi esperimenti, le HUVEC sono state coltivate in piastre multi-well standard utilizzando gli stessi protocolli di coltura applicati nel chip microfluidico. Per valutare se la tossicità degli antagonisti potesse avere un effetto sinergico con il TNF- α , abbiamo effettuato un trattamento con gli antagonisti da soli o dopo esposizione al TNF- α .

Risultati e discussione

I risultati del saggio di immunofluorescenza hanno mostrato che l'espressione di ICAM-1 era stimolata all'aumentare dello shear stress rispetto al controllo statico. Al contrario, le cellule endoteliali in condizioni statiche non esprimevano questa molecola di adesione. D'altra parte, VCAM-1 era espressa a livelli molto bassi e sembrava che l'espressione diminuisse con l'aumentare della portata rispetto al controllo statico. Per testare l'influenza della stimolazione pro-infiammatoria, abbiamo valutato l'espressione di ICAM-1 e VCAM-1 nelle cellule endoteliali

mantenute in condizioni statiche o soggette a portata di 30 $\mu\text{L}/\text{h}$, entrambe in presenza o in assenza di TNF- α . I risultati hanno evidenziato che l'espressione di queste molecole di adesione era sovraregolata dopo l'esposizione al TNF- α rispetto alla condizione senza TNF- α . In particolare, il TNF- α ha stimolato l'espressione di ICAM-1 più in dinamico (30 $\mu\text{L}/\text{h}$) che in condizioni statiche, suggerendo un effetto sinergico tra flusso e TNF- α . D'altra parte, VCAM-1 era sovraregolato in presenza di TNF- α più nella condizione statica che nei campioni sottoposti a condizioni dinamiche, confermando la tendenza osservata solo con il flusso. Alla luce di questi risultati, abbiamo selezionato la condizione dinamica che ha indotto la maggior espressione delle due molecole di adesione. Pertanto, per gli esperimenti successivi, il monostrato endoteliale è stato pre-condizionato con flusso di fluido a 30 $\mu\text{L}/\text{h}$ e TNF- α (Fig. 2).

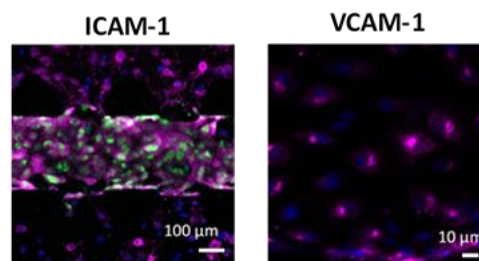


Fig. 2 - Immagini che mostrano l'espressione di ICAM-1 e VCAM-1 nelle cellule endoteliali sottoposte a TNF- α con perfusione a 30 $\mu\text{L}/\text{h}$

Gli esperimenti per la validazione del modello hanno mostrato che l'extravasazione dei monociti era direzionale verso il canale delle chemochine, confermando che l'extravasazione osservata era specifica e guidata dal segnale delle chemochine. Come atteso, l'extravasazione dei monociti in presenza del mezzo di controllo era praticamente assente. Al contrario, un numero elevato di monociti è extravasato in risposta alla mix di chemochine. Inoltre, abbiamo verificato che dopo il pre-condizionamento dell'endotelio il numero di cellule extravasate era più alto rispetto ai chip statici, suggerendo che il pre-condizionamento simulasse meglio le condizioni *in vivo* (Fig. 3).

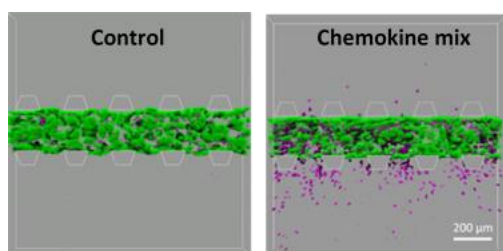


Fig. 3 - Ricostruzione 3D di immagini confocali che mostrano l'extravasazione dei monociti in risposta al mezzo di controllo o ad una miscela di chemochine dopo il pre-condizionamento con flusso di 30 $\mu\text{L} / \text{h}$ combinato con $\text{TNF-}\alpha$

I saggi di extravasazione successivi hanno mostrato che i monociti sono extravasati in presenza di liquido sinoviale di pazienti con OA, mentre in presenza del mezzo di

controllo sono rimasti confinati all'interno del canale endoteliale, dimostrando l'effetto chemoattraente del liquido sinoviale. L'extravasazione direzionale verso il compartimento inferiore indotto dal liquido sinoviale era significativamente maggiore rispetto a quella non specifica verso il compartimento superiore in tutte le condizioni testate (Fig. 4).

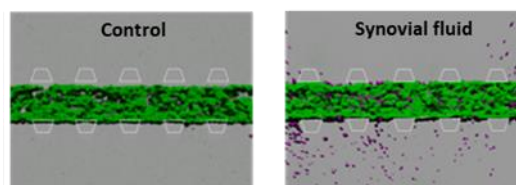


Fig. 4 - Ricostruzione 3D di immagini confocali che mostrano l'extravasazione dei monociti in risposta al mezzo di controllo o al liquido sinoviale dopo il pre-condizionamento con flusso di fluido di 30 $\mu\text{L} / \text{h}$ combinato con $\text{TNF-}\alpha$

Sorprendentemente, i monociti sono extravasati in maggior numero nel sistema senza le cellule di supporto (SFb e ACh) rispetto all'extravasazione osservata nel sistema completo. Questi risultati hanno indicato che SFb e ACh hanno un ruolo nel processo di extravasazione, rendendo il sistema completo più simile alle condizioni *in vivo* rispetto a un sistema semplificato.

Per quanto riguarda i risultati dei test di citotossicità, è emerso che tutti gli antagonisti hanno avuto un effetto citotossico sulle HUVEC, che è diminuito a

concentrazioni di antagonista più basse. Inaspettatamente tutti gli antagonisti combinati insieme, hanno avuto un effetto citotossico inferiore rispetto ai singoli antagonisti. Anche la citotossicità di CVC sembrava inferiore rispetto ai singoli antagonisti, rendendolo un antagonista promettente da utilizzare nel nostro dispositivo. Le HUVEC trattate anche con TNF- α hanno mostrato complessivamente una minore citotossicità in risposta al singolo antagonista o agli antagonisti combinati tutti insieme comparate alle HUVEC non esposte al TNF- α . Questi dati preliminari verranno utilizzati in futuro per ottimizzare le condizioni sperimentali per testare gli antagonisti e valutare la loro abilità per inibire l'extravasazione dei monociti nel nostro modello microfluidico.

Conclusioni e prospettive future

In questa tesi, abbiamo convalidato un dispositivo organotipico microfluidico che modella il processo di extravasazione dei monociti in un'articolazione affetta da OA. Abbiamo ottimizzato i parametri di pre-condizionamento e valutato l'extravasazione dei monociti in

risposta a un mix di molecole chemoattrattive note o al liquido sinoviale derivato da pazienti. Nel prossimo futuro, i risultati ottenuti nei test di citotossicità verranno applicati per usare il chip come piattaforma per la selezione di farmaci anti-chemochine.

References

1. Glyn-Jones, S., Palmer, A. J. R., Agricola, R., Price, A. J., Vincent, T. L., Weinans, H., & Carr, A. J. (2015). Osteoarthritis. *The Lancet*, 386(9991), 376-387
2. Berenbaum, F. (2013). Osteoarthritis as an inflammatory disease (osteoarthritis is not osteoarthrosis!). *Osteoarthritis and cartilage*, 21(1), 16-21.
3. Kapoor, M., Martel-Pelletier, J., Lajeunesse, D., Pelletier, J. P., & Fahmi, H. (2011). Role of proinflammatory cytokines in the pathophysiology of osteoarthritis. *Nature Reviews Rheumatology*, 7(1), 33.
4. K. Ley, C. Laudanna, M. I. Cybulsky e S. Nourshargh, *Getting to the site of inflammation: The leukocyte adhesion cascade updated*, vol. 7, 2007, pp. 678-689.

5. Schenkel, A. R., Mamdouh, Z., & Muller, W. A. (2004). Locomotion of monocytes on endothelium is a critical step during extravasation. *Nature immunology*, 5(4), 393
6. Barr, A. J., & Conaghan, P. G. (2013). Disease-modifying osteoarthritis drugs (DMOADs): what are they and what can we expect from them. *Medicographia*, 35, 189-196.
7. M. A. Karsdal, M. Michaelis, C. Ladel, A. S. Siebuhr, A. R. Bihlet, J. R. Andersen, H. Guehring, C. Christiansen, A. C. Bay-Jensen e V. B. Kraus, «Disease-modifying treatments for osteoarthritis (DMOADs) of the knee and hip: lessons learned from failures and opportunities for the future,» *Osteoarthritis and Cartilage*, vol. 24, n. 12, pp. 2013-2021, 2016.
8. Chen, H. C. (2005). Boyden chamber assay. In *Cell migration* (pp. 15-22). Humana Press
9. Bhatia, S. N., & Ingber, D. E. (2014). Microfluidic organs-on-chips. *Nature biotechnology*, 32(8), 760

1. Introduction

1.1. Osteoarthritis

1.1.1. General description

Osteoarthritis (OA) is a degenerative joint disease and the most common form of arthritis. It could affect any joint but usually the most common are knees, hips, hands and spinal joints. Generally, it is characterized by joint pain during movements, stiffness, loss of flexibility and swelling causing a huge impact in patient life, making OA as one of the most debilitating disease. Millions of people in the world are affected by OA and the number of patients is going to increase due to the aging of population and to the growth of obesity [1].

Several risk factors are associated to this pathology and can be divided in systemic and local factors. Among the systemic factors, age is the strongest one: as it increases, all joints have a greater probability to develop OA, since different biological changes arise with age, such as lower tissue regeneration, cartilage thinning and oxidative damage. Another systemic factor is gender, indeed it has been reported that women are more subjected to suffer of OA than men. Among the local factors, obesity plays a major role, not only for the greater mechanical loading to which they are subjected but also for metabolic factors [2]. Recent studies showed that obesity can be considered as a chronic low-grade inflammatory disease with consequent altered levels of pro-inflammatory cytokines [3]. Other risk factors are genetic, previous joint injuries, joint alignment and diet, indicating the complexity to find a main cause for this disease [2, 4].

1.1.2. Synovial joint

Synovial joints are the most common type of joint in the body. Synovial joints are characterized by a joint cavity and a fluid-filled space in which the articulating surfaces of bones are in contact each other. The inner surface of the joint capsule is lined by synovial membrane which produces the synovial fluid that fills the joint cavity and lubricates the joint [5].

Synovial joints allow a wide degree of movements like translation, rotation, flexion, and extension. Synovial joint is a complex anatomical structure composed of different elements: synovial membrane, articular cartilage, synovial fluid, articulating bones, periosteum and in some cases other additional structure such as accessory ligaments, tendons, articular disc, and bursae. A representation of synovial joint is shown in Figure 1.

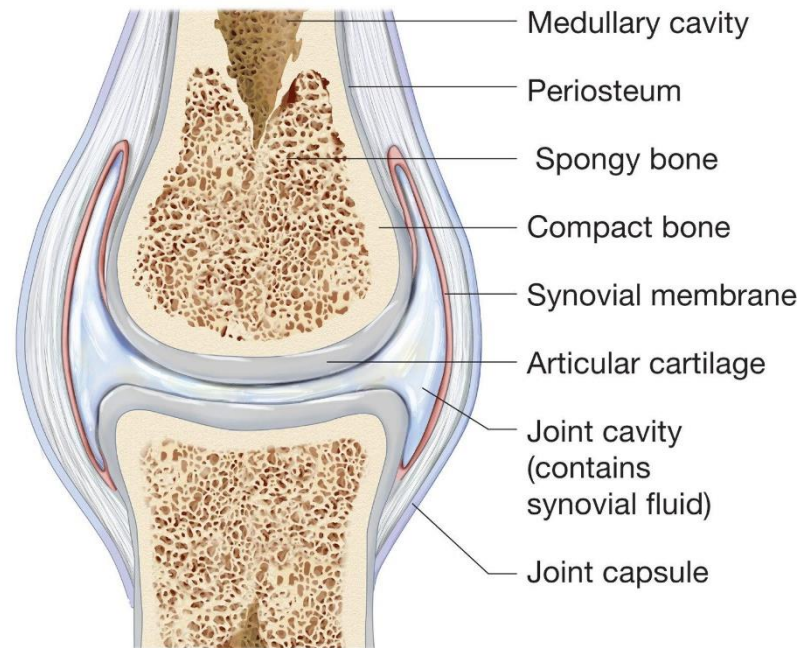


Figure 1 – Internal structure of a synovial joint. (source: www.pdhpe.net)

1.1.3. OA as a whole-joint disease

For a long time OA has been considered as simple wear and tear disease involving only the degeneration of the cartilage with a collateral impact on the surrounding tissues, such as synovial membrane and subchondral bone. Recent studies suggested not to consider OA as simple cartilage pathology but as a whole-joint disease, since all joint tissues contribute to disease progression [6, 7]. Specifically, an OA joint is characterized by synovial membrane inflammation and stiffening, articular cartilage degradation, decreased viscosity of the synovial fluid, subchondral bone thickening and osteophytes formation (Figure 2) [8, 9].

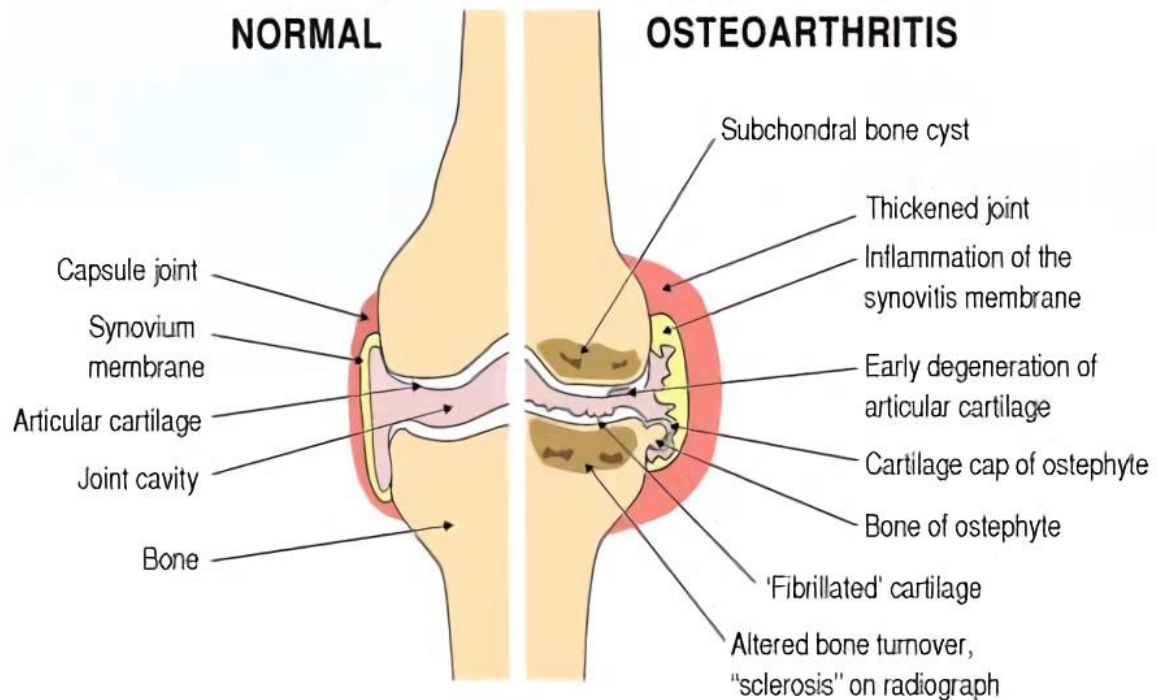


Figure 2 - Structural difference between healthy (left) and OA joint (right) [source <https://www.creative-biolabs.com>]

Even though it is still unknown the sequential events that occur in the pathogenesis of OA, it is known that the inflammation of the synovial tissue is one of the major components that drives the progression of this disease. During inflammation process, the production of different cytokines, such as Tumor Necrosis Factor- α (TNF- α) and Interleukin-1 β (IL-1 β), is increased, thus inhibiting the synthesis of extracellular matrix (ECM) from chondrocytes. In addition, these cytokines stimulate the chondrocytes to produce matrix metalloproteinases (MMPs), such as MMP-1, MMP-3 and MMP-13, which regulate the destruction of cartilage ECM. Moreover, cytokines stimulate the release of nitric oxide and prostaglandin E₂ that contribute on amplifying articular inflammation and degeneration by inducing in turn MMPs synthesis and inhibiting the production of macromolecules, such as collagen. Additionally, TNF- α and IL-1 β activates different signaling pathways, including the most important through nuclear factor κ B (NF κ B). It mediates the expression of inflammatory genes that encode for nitric oxide synthetase and chemokines which are involved in the recruitment of monocytes and macrophages, bringing to their accumulation in the synovial tissue. In turn, macrophages produce additional pro-inflammatory cytokines that amplifies the inflammation response, leading to a chronic inflammation [10].

Currently, there is a lack of treatments inhibiting the joint deterioration in OA patients and drugs are directed only to alleviate pain and symptoms without counteracting OA progression. Long-term management of the disease include healthy diet and exercise. Up to now, patients inevitably undergo total joint replacement because of the progressive degeneration of the joint. Therefore, in recent years novel chemical agents known as disease-modifying osteoarthritis drugs (DMOADs) have been developed. These kinds of drugs might target cartilage, inflammation or subchondral bone to inhibit OA progression, improve the tissue function and alleviate the symptoms [11]. As an example, PG-116800 inhibits the action of MMPs preventing cartilage degradation but clinical trials failed because it induced musculoskeletal adverse reactions. Other DMOADs as AMG-108 acts on inflammation process. This anti-cytokine drug can target TNF- α causing a down-regulation of MMPs, although clinical trials showed no significant difference between treatment and placebo. Even though there are different DMOADs that may counteract OA progression, neither of them has showed positive clinical results [12]. Anti-chemokine drugs targeting chemokine signaling involved in recruitment of monocytes and macrophages may represent a novel strategy to prevent macrophages accumulation in the synovial membrane, thus limiting progression of inflammation during OA. Moreover, these drugs could represent a novel therapy for obese patients. Indeed, a recent study by Krinniger et al. showed that obese individuals have an increase in percentage of CD14+/CD16+ monocytes with a superior migration ability [13].

1.1.4. Inflammation

Inflammation is a defense response of vascularized tissues to injury of any kind. It is a fundamental defense reaction with the main aim of eliminating the primary inflammatory trigger, thus contributing to tissue repair [14]. It is part of the innate immune system and an initiator and regulator of the adaptive immune system [15]. This process is commonly initiated by micro-organisms or damaged/dead cells or in response to tissue and/or cellular stress [16]. Inflammation occurs in the microvasculature of the affected tissue, and the main process is leukocyte extravasation (diapedesis) from post-capillary venules into surrounding tissues [15]. In particular, monocyte extravasation involves a series of

sequential steps, which are tethering, rolling, adhesion and trans-endothelial migration (TEM). Once leukocytes extravasated, they migrate through the ECM along a concentration gradient of inflammatory molecules [17].

Extravasation is an active and highly regulated process that involves both leukocytes and endothelial cells and is mediated by adhesion molecules which drive the process of diapedesis. The adhesion molecules are expressed on both endothelial cells and leukocytes. As described by Ley et al., there are three main families of adhesion molecules: selectins, integrins, and immunoglobulins. Selectins mediate the rolling of leukocytes on the endothelial monolayer. In particular, L-selectin, P-selectin and E-selectin interact mainly with P-selectin glycoprotein ligand 1 (PSGL1), which is a selectin ligand found mainly on leukocytes and allows the recruitment of monocytes by activated endothelial cells [18]. L-selectin is expressed mostly by leukocytes while P-selectins and E-selectins by inflamed endothelial cells. PSGL1 interacts with L-selectin prompting leukocyte-leukocyte binding which in turn favors secondary leukocyte capture. This interaction allows the adhesion of leukocytes that do not express ligands for E-selectin and P-selectin [19]. Subsequently, integrins on leukocytes bind to immunoglobulins expressed by endothelial cells and play a crucial role in TEM process because they participate in the rolling phase and allow the firm adhesion of leukocytes on the monolayer. The two main immunoglobulins are the intercellular adhesion molecule-1 (ICAM-1) and vascular cell adhesion molecule-1 (VCAM-1) (Figure 3) [19]. The final step is the transmigration through the endothelial monolayer and can happen in two ways: paracellular or transcellular migration. The most common way is the paracellular migration, in which leukocytes crawls on the endothelial monolayer scanning for exit cues, chemoattractant agents and ICAM-1 play a crucial role enabling leukocytes to crawl inside cellular junction and transmigrate. At this point chemokines

guide leukocytes to pass the basement membrane leading them to the inflammation site [16].

During inflammation, endothelial cells are activated by inflammatory cytokines to increase expression of adhesion molecules and chemokines that are presented on luminal surface. Moreover, endothelial cells transport exogenous chemokines from abluminal to luminal surface presenting them to leukocytes, thus inducing extravasation process [20]. Although leukocyte recruitment is fundamental for initiating tissue healing, an alteration of the process can amplify the inflammatory response, generating a pathologic condition instead of repairing the tissue. For instance, monocyte infiltration, their sub-endothelial accumulation, and differentiation into macrophages is a crucial point in the pathogenesis of OA. In fact, during OA accumulated macrophages release pro-inflammatory cytokines which stimulate the production of chemokines and consequently the recruitment of more monocytes leading to chronic inflammation [15]. Therefore, an approach aimed to decrease monocytes extravasation would help to decrease the inflammation, thus OA progression.

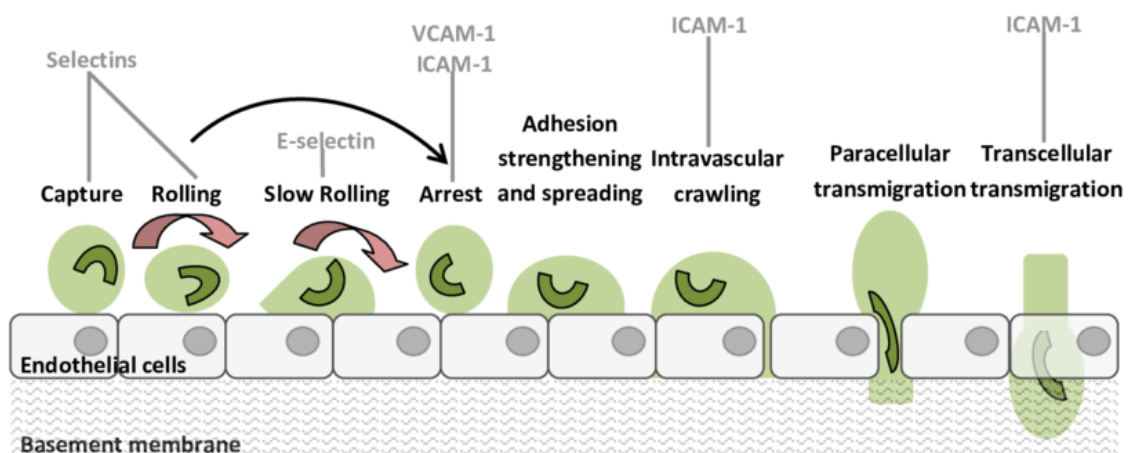


Figure 3 – Representation of the extravasation process, showing in each phase the adhesion molecules involved. In response to a diverse range of proinflammatory triggers, that can stimulate leukocytes and vascular cells to initiate a cascade of leukocyte adhesion and motility responses. This enables optimal scanning of the vascular lumen for exit signals. Leukocyte rolling, firm attachment, and intravascular crawling are sequentially mediated by the indicated endothelial cell adhesion molecules and leukocyte endothelial selectin and integrin ligands, responses that are prerequisites to leukocyte migration through venular walls. A delicate balance between integrin-ligand microclusters allows arrested leukocytes to scan the endothelial lumen for chemotactic exit signals under hydrodynamic forces.

1.1.5. Involved tissues

1.1.5.1. Articular cartilage

Articular cartilage is a highly specialized connective tissue of the synovial joints. Its principal function is to provide a smooth, lubricated surface for articulation and to facilitate the transmission of loads with a low frictional coefficient. Articular cartilage is not vascularized, not innervated and without lymphatic structures, therefore it receives nutrients and oxygen by synovial fluid and subchondral bone [21].

Water is the most abundant component of articular cartilage, constituting up to 80% of wet weight. The remaining solid phase is formed by extracellular matrix (ECM) and chondrocytes. ECM is composed of collagen fibers, aggrecan, and proteoglycans [22]. Collagen is the main structural macromolecule in ECM and constitutes about 60% of dry weight of cartilage. In particular, type II collagen represents 90% to 95% of the total collagen of ECM. Other collagen types contribute only in minor proportion [23]. Since the permeability of the ECM is very low, compression of the matrix causes pressurization of the water within the matrix, leading to the articular cartilage the ability to withstand significant loads, together with the frictional resistance to water flow [23]. Chondrocytes constitute about 5% of articular cartilage and play a fundamental role in development and maintenance of the ECM, synthesizing matrix components and enzymes for homeostasis of ECM [23].

It is possible to divide articular cartilage in four different zones from top to bottom:

1. Superficial zone: thin layer of flattened ellipsoid chondrocytes that synthesize high concentration of collagen and low amounts of proteoglycans. Parallel fibrils provide the greatest tensile and shear strength. Disruption of this zone alters mechanical properties of articular cartilage, contributing to the development of OA. This layer is in direct contact with synovial fluid.
2. Middle (or transitional) zone: spheroid-shaped cells at low density. Collagen fibers are randomly arranged with higher concentration of aggrecan.
3. Deep zone: cells are arranged perpendicular to the surface with the lowest concentration. This is the zone with the highest concentration of aggrecan and the largest diameter of collagen fibers.

4. Calcified cartilage zone: very low density of cells embedded in calcified matrix, showing a very low metabolic activity.

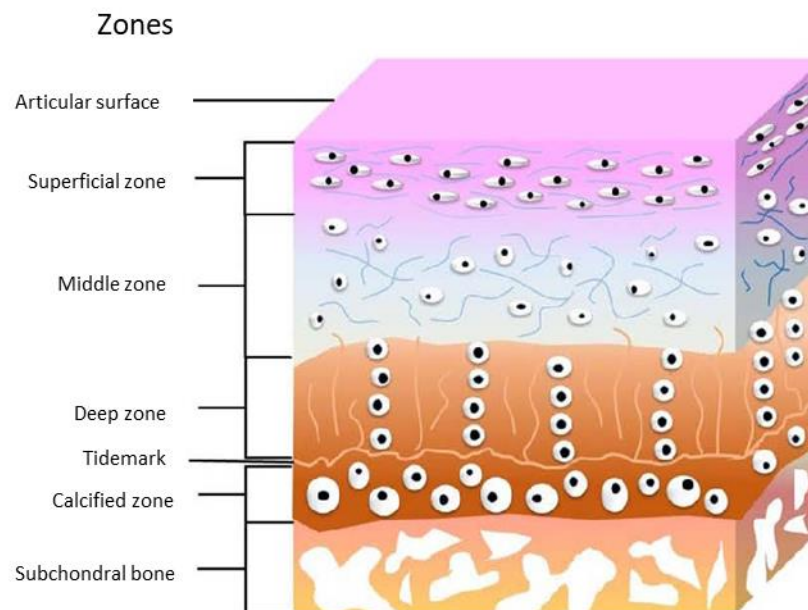


Figure 4 – Schematic representation of articular cartilage, showing all the zones that constitute it. From top to bottom it is possible to distinguish the superficial, middle and deep zone. [source: <https://www.semanticscholar.org>].

During OA progression, the ECM of articular cartilage is degraded by MMPs produced by chondrocytes. Indeed, inflammatory cytokines induce metabolic changes in chondrocytes, especially in the upper zone, downregulating the synthesis of ECM and amplifying the catabolism by increasing the production of MMPs. Due to the increased permeability and disruption of the ECM, the water content reaches 90%, leading to decreased elasticity and thus to reduction of load-bearing capability of the articular cartilage [21].

1.1.5.2. Synovial membrane

The joint capsule is formed by a dense fibrous connective tissue, which seals the joint space. This connective tissue has different functions, that is keeping the lubricating synovial fluid in position inside the joint and providing passive stability by limiting the movements. Like all connective tissues, the joint capsule is vascularized and innervated [24].

The joint capsule consists of an outer fibrous layer and an inner synovial layer called synovial membrane or synovium. The synovial membrane is a thin layer of very few cells. It consists of three different cell types: synovial macrophages, synovial fibroblasts, and

dendritic cells. This highly vascularized layer secretes synovial fluid and regulates the metabolism of articular cartilage by acting as selectively permeable membrane [25].

In OA patients, synovial tissues are characterized by infiltration of macrophages, expression of pro-inflammatory cytokines, intensification of micro-vascular network and increasing of fibrous tissue [8].

1.1.5.3. Synovial fluid

Synovial fluid plays a very important role in the synovial joint since it transports nutrients to the avascular articular cartilage and supports the mechanical function of the joint by lubricating the articular surfaces. The synovial fluid is an ultrafiltrate of blood plasma and contains proteins both derived from plasma and produced by cells of the joint [26]. It contains low molecular weight solutes such as oxygen, carbon dioxide and glucose, which can diffuse freely through the endothelium of the synovial membrane, and high weight proteins, such as lubricin and hyaluronan. Lubricin is a glycoprotein determining the lubricating capacity of the synovial fluid, while hyaluronan is the major proteoglycan responsible for the high viscosity of synovial fluid, determining also its non-Newtonian behavior [25]. In pathological conditions, such as inflammatory and degenerative diseases, the composition of synovial fluid can be altered due to a reduction of molecular weight and concentration of hyaluronic acid, decreasing its lubricating properties [27].

1.2. Microfluidics

1.2.1. General principals

Microfluidics is the science of manipulating and controlling fluids in channels with dimensions of tens of micrometers. Microfluidic technology has its origin around 1975, when the first miniaturized gas chromatography system was created. Only after 1991 the advantages of microfluidics were thrust into the attention, especially for its application in chromatography [28]. The large possibility of integration of microfluidic allowed to reach the goal to be able to detect biological molecules, and transport, mix and to analyze raw samples. This achievement introduced the concept of 'Lab-on-a-chip' systems: devices that integrates in a single chip several analyses that usually are done in a laboratory [29].

The benefits that miniaturization offers are various [30]:

- Reduction of timing like transport time, diffusion time and detection time
- Very low fabrication costs
- Reduction of sample and reagents required
- Compact systems
- High-throughput analyses
- Ability to control the environment of cell culture spatially and temporally
- Possibility to control single-cell behavior by means of high quality and time-lapse imaging

The effects that become dominant in microfluidics include laminar flow, surface area to volume ratio, diffusion, and surface tension. Below, each factor is briefly described:

- *Laminar flow*: The Reynolds number (Re) is the ratio between inertial and viscous forces, and it is a dimensionless number. It indicates the type of flow. If Re is smaller than 2000, the flow is laminar, it means the fluid lines are parallel one to each other; between 2000 and 4000 the flow is transitional; and over 4000 the flow is turbulent, meaning that the inertial forces prevail on the viscous forces. The equation to calculate Re is:

$$\text{Re} = \frac{v D \rho}{\mu} \quad (\text{Eq. 1})$$

Where ρ is the fluid density, v is the characteristic velocity of the fluid, μ is the fluid viscosity and D is the hydraulic diameter. Usually, in macroscale systems it is very difficult to have a laminar flow. Conversely, in microscale systems it is possible to obtain the Reynolds number around 1, meaning that it works always with laminar

flow (Figure 5). To reach a turbulent flow in a microscale system, it is necessary to use very high pressures [31].

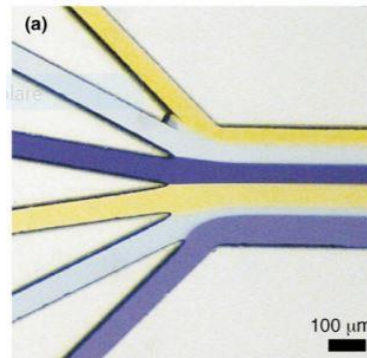


Figure 5 – Laminar streams of solutions of dye (in water) flowing in microfluidic channels. The fluid is flowing from the six channels on the left into the central channel on the right where flow is laminar [32].

- *Surface area to volume ratio and diffusion:* Moving from macro-scale towards micro-scale systems, surface area to volume ratio increases substantially since the surface area is proportional to r^2 , while the volume is proportional to r^3 . As a result, the surface forces become more significant than body forces, which in turn makes the diffusive phenomena significant to a great extent since the amount of surface exposed to a volume of fluid increases notably [32].

As a result of the laminar flow, increased surface area and diffusion play a pivotal role in microfluidics. Indeed, due to the laminar flow molecules do not mix and the diffusion in microscale systems has a very high rate, contrary to the macroscale diffusion. Diffusion is a non-linear process and the time t that a molecule requires to diffuse through a given distance x can be modeled in one dimension by the equation:

$$x^2 = 2Dt \quad (\text{Eq. 2})$$

Where x is the distance that a particle moves in a time t , and D is the diffusion coefficient of the particle. From the equation 2, it is clear that diffusion at micro and nano scale is a very efficient mixing method, while at the macroscale is very inefficient. For example, taking into account a small molecule, which diffusion coefficient is typically $5 \times 10^{-10} \text{ m}^2/\text{s}$, it will take 0.1 s to diffuse through 10 μm , 10 s for 100 μm and 27 h for 1 cm [33]. Since the distance varies with the square power,

at the microscale the diffusion times are shorter and consequently, diffusion phenomenon become dominant, being in many cases used as an efficient mechanism of mixing [33].

- *Surface tension*: in a liquid due to cohesive forces every molecule is pulled in every direction by neighbor molecules, resulting in zero net force. Molecules situated at the surface are not pulled in every direction since they are not completely surrounded by other molecules, therefore this results in a force that pulls inside the molecules. At the micro scale it results more relevant, but it can be considered more a disadvantage because if we consider having an empty branched tube that has to be filled with water, if a branch is not filled completely it can lead to the device failure due to the Laplace pressure (Eq.3). Because pressure difference increases with the decrease of radius of the liquid.

$$\Delta P = \frac{2\gamma}{R} \quad (\text{Eq. 3})$$

1.2.2. Manufacturing of microfluidic devices

Microfabrication technologies are essential tools in various fields such as microelectronic and micro-analytical systems. Lithographic technologies allow to transfer a specific pattern to a surface [34]. Photolithography is the most widely used form of lithography and allows to transfer the desired pattern using light onto a photosensitive polymer. In particular, the most used technique to obtain microfluidic devices for biomedical applications is soft lithography. The term soft lithography refers to a set of techniques used for the reproduction of micro and nano-structured surfaces using elastomeric materials. These techniques include Micro Contact Printing (μCP), Micro Molding in Capillaries (MIMIC) and Replica Molding [35]. The most used material for the fabrication of microfluidic devices by soft lithography is an inorganic silicon-based polymer named polydimethylsiloxane (PDMS). The PDMS structure contains a siloxane group and methyl groups (Figure 6). PDMS has a

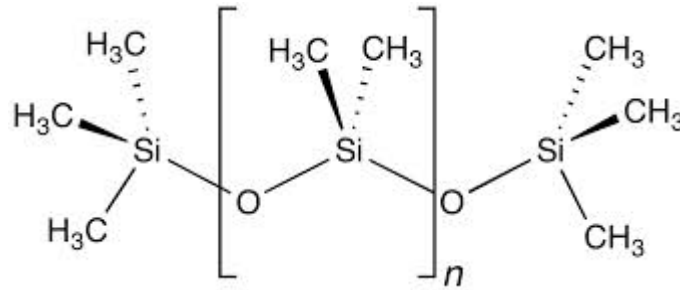


Figure 6 - Basic monomeric unit of polydimethylsiloxane [source: www.elveflow.com].

useful combination of properties, such as a Young's modulus that makes it a moderately stiff elastomer (1 MPa), non-toxic, making it suitable to be in contact with cells, and it is optically transparent allowing high-quality imaging [36]. It is also gas permeable, allowing an appropriate diffusion of O₂ and CO₂. Another favorable characteristic of PDMS is its thermal stability, which renders it autoclavable for sterilization. Furthermore, due to the presence of methyl groups, plasma treatment renders its hydrophobic surface temporarily hydrophilic in order to bond it onto glasses. Finally, it is relatively cheap and available in commerce in ready to use formulations, it is easy to mold and offers rapid prototyping capabilities of microfluidic devices [37].

Despite all these advantages, PDMS has also some unfavorable characteristics that may limit its functionality in cell culture assays:

- Deformation: the high compliance of PDMS can determine an undesired deformation of microchannels. For instance, PDMS may bulge when the pressure inside the channel is very high or may sag due to its weight when the ratio between the height and the width of the channel is too low;
- Shrinkage: after the reticulation, PDMS shrinkage is about 1.7%. This issue can be easily solved increasing the dimensions of the device in the starting design
- Evaporation: PDMS is extremely permeable to water vapor and, at the microscale, evaporation can become an important issue, causing the formation of bubbles that can block the flow and lyse the cells
- Absorption: unlike materials as thermoplastics and glass that are only subject to surface absorption, PDMS is a permeable material with the tendency to bulk non-specific absorption of hydrophobic compounds

- Leaching: residual uncrosslinked oligomers can leach out from the bulk and then bind to cell membranes, affecting cell metabolism and proliferation
- Hydrophobic recovery: PDMS polymer chains can diffuse from the bulk to the surface, replacing hydroxyl groups created by the oxygen plasma treatment allowing the bonding with glass coverslips. In addition, the effects of plasma treatment have a limited shelf life due to the gradual reversal of hydrophilicity [38, 39].

Figure 7 recapitulates the three phases of soft lithography:

1. *Concept developing:*

CAD software (AutoCAD, Autodesk) is used to realize the microfluidic design according to the specifications. The CAD pattern is printed at high resolution, generating black regions on a transparent film that is then used as photomask.

2. *Rapid prototyping:*

A polymeric material sensible to light source is spin-coated on a silicon wafer as a photoresist and once deposited, it is exposed to UV light through a photomask that works as selective filter. Later on, the uncrosslinked areas of the photoresist are removed by a developer solution to obtain the silicon master mold. Based on the class of the photoresist which can be positive or negative, masks used for transferring the patterns are different. In positive photoresists the designed mask replicates an exact copy of the pattern remaining on the silicon wafer master. Conversely, with the negative photoresist unexposed areas to the UV light are removed and as result, negative of the pattern will be transferred.

3. Replica molding:

The obtained silicon master can be considered as a negative copy of the desired pattern. PDMS is poured on the silicon wafer and after polymerization, it is peeled off. Then, biopsy punchers of desired diameters are used to obtain input and output ports. Finally, to obtain enclosed channels, the chip is bonded on a surface such as glass coverslip or another PDMS layer.

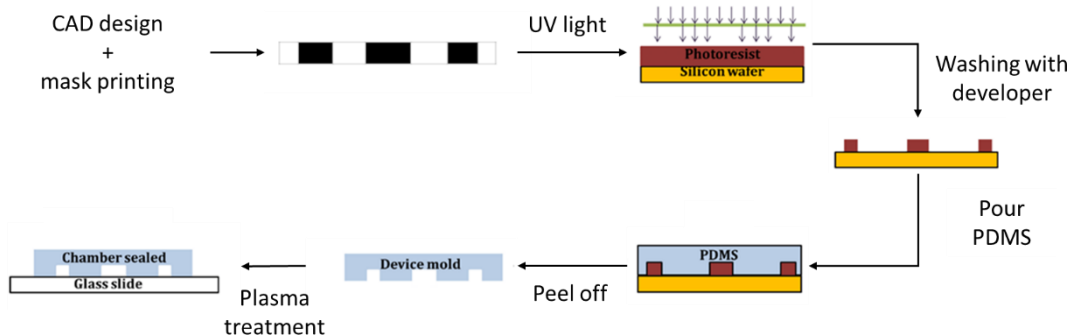


Figure 7 - Schematic representation of the soft lithographic procedure for the realization of PDMS microfluidic devices

1.2.3. Microfluidics in biological applications

Considering all the benefits that provides, microfluidics has recently been used extensively in biological research. Indeed, microfluidics allows to time exactly fluid flow using in-chip valves and to precisely have chemical and physical control of the microenvironment [40]. In addition, it is possible to move from classical 2D to 3D cell culture, in which cells are supported in all directions by other cells and ECM. Cells cultured in 3D environment display a gene expression profile and biological activity that resemble the *in vivo* situation more closely than 2D culture [41]. Furthermore, microfluidic platforms used for cell culture have the potential to mimic *in vivo* cellular microenvironment (composed of physical, biochemical, and physiochemical factors) with high spatial and temporal precision. For instance, the possibility to create a biomimetic molecular gradient within the microfluidic chips has made it possible to study some fundamental processes such as inflammation and cell migration.

In the last decades, hydrogels have demonstrated promising efficiency to be used as scaffolds for 3D cell culture. Hydrogels supply biochemical and structural cues that

resemble critical aspects of natural ECM, allowing easy transport of oxygen, nutrients, waste, and soluble factors. Among natural and synthetic scaffolds, fibrin hydrogel is widely used in biological research due to its high biocompatibility, short polymerization time and flexible properties. For instance, tuning the fibrinogen or/and thrombin concentration.

Fibrin in the organism plays a crucial role in blood clotting, wound healing process, and it is strictly connected to fibrinogen. During an injury the soluble molecule of fibrinogen, precursor of fibrin, is cleaved by thrombin as part of an enzymatic cascade. Once cleaved the fibrinogen is able to form cross-link between other cleaved molecules of fibrinogen, in this way an insoluble network of fibrils of fibrin is formed promoting blood clotting. Fibrin is widely used in different applications especially in tissue engineering and regenerative medicine.

Another important advantage of microfluidics it is the possibility of co-culturing different types of cells in the same device, allowing to resemble specific tissues and organs, producing so-called organs-on-chips. Organ-on-chip systems are microfluidic devices for culturing living cells in continuously perfused micrometer-sized chambers in order to model physiological functions of a tissue or organ (Figure 8). The objective is to resemble the essential functions that characterize tissue or organ behavior. These types of systems can provide different stimuli to the involved cells based on the tissue or organ we want to resemble. For instance, it is possible to apply a specific shear stress, mechanical

compression or cyclic strain. These systems allow to have a tissue or organ specific response in reaction to drugs, toxins or other environmental perturbations [42].

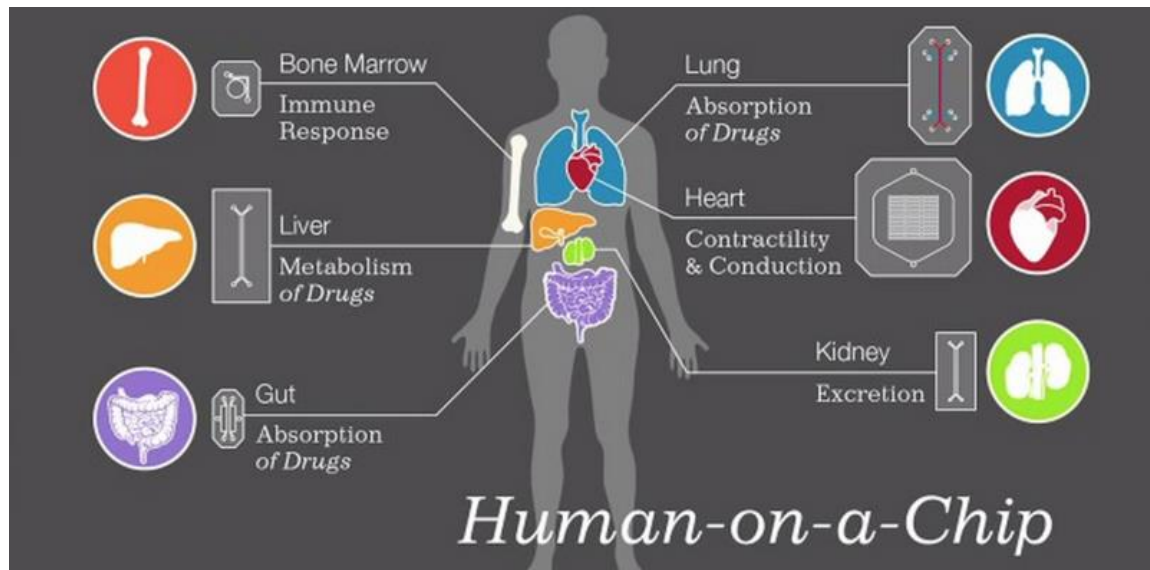


Figure 8 - Examples of organ-on-a-chip

1.2.4. Models of OA

Joints are complex multi-tissue organ composed of cartilage, synovial membrane and bone. Therefore, it is difficult to have a model able to replicate joints as close as possible. During OA macrophages accumulates in the synovial tissue releasing pro-inflammatory cytokines, like $\text{TNF-}\alpha$ and $\text{IL-1}\beta$, which induce the production of catabolic proteins causing the degradation of the ECM of the cartilage. The complicate interactions among all the joint tissues make the creation of a joint model difficult, and consequently the study of OA [43]. Considering the complexity of articular joints, to mimic it as close as possible a model should consider different aspects, including interactions among the involved tissues and mechanical stimulation. Both 2D and 3D *in vitro* models have been developed to study OA joints. Up to now, the majority of OA studies focused on models based on cartilage cells, due to their rapid response to cytokines and mechanical stimuli and for the easier use as a monolayer [44]. For instance, Lin et al. co-cultured chondrocytes and osteoblasts showing that osteoblasts subjected to high mechanical stress, similar to OA condition, induced chondrocytes to increase expression of different MMPs. Conversely, when chondrocytes were co-cultured with unstressed osteoblasts, they shifted to hypertrophic phenotype

reducing collagen type II, suggesting that osteoblasts stressed with high mechanical compression modify adjacent cartilage by increasing MMPs synthesis and by inhibiting ECM production. Changes that are similar in an OA joint [44]. In another model developed by Beekhuizen et al. synovial tissue and cartilage both derived from OA patients were co-cultured. It demonstrated that the synovial tissue influenced the cartilage metabolism by lowering the expression of glycosamino-glycan (GAG). Moreover, it showed that the inhibition of cytokine production and activity of MMPs can counteract the decrease of GAG, indicating anti-cytokine drugs as a possible solution [45]. Occhetta et al. developed a cartilage-on-chip model that allowed the application of 3D strain-controlled compression, inducing OA traits to the cartilage compartment. Indeed, the application of hyper-physiological compression on healthy cartilage induced loss of cartilage matrix, increase of inflammation, production of degrading mediators and acquisition of hypertrophic traits [46].

1.2.5. Extravasation models

In order to have an insight of the basic process of inflammation during OA, it is necessary to study the extravasation of the leukocytes towards synovial membrane and their interaction with the endothelial cells. Several *in vitro* models have been developed to study this process, such as the Boyden chamber that is a transwell system with a porous membrane on which endothelial cells are cultured to form a monolayer. Leukocytes are placed inside and allowed to migrate through the pores driven by chemoattractant agents placed in the lower chamber [47]. Even though this *in vitro* assay contributed a lot in understanding the diapedesis process, it has some limitations. Indeed, the chemokine gradient is unpredictable over space and time [48] and the assay is performed in static conditions, meaning that there is a lack in considering the importance of the physiological flow and shear stress, fundamental for expression of adhesion molecules involved in extravasation process. Moreover, the Boyden chamber is highly affected by gravity that induce leukocytes to migrate even without e chemoattract stimulus [49, 50].

It is clear that this system could not represent completely the *in vivo* condition, thus it is necessary to take into account a system which can reproduce as close as possible the physiological condition. For this purpose, microfluidics has many characteristics that can overcome the above-mentioned disadvantages. Several microfluidic devices have been developed, such as the one designed by Han et al., which includes an endothelial monolayer to study the migration of neutrophils in response to a chemotactic stimulus. Although it allows to study neutrophils extravasation, it lacks on considering the effects of shear stress and the presence of supporting cells, as SFb and ACh, fundamental if we want to resemble as close as possible a synovial joint (Figure 9) [51].

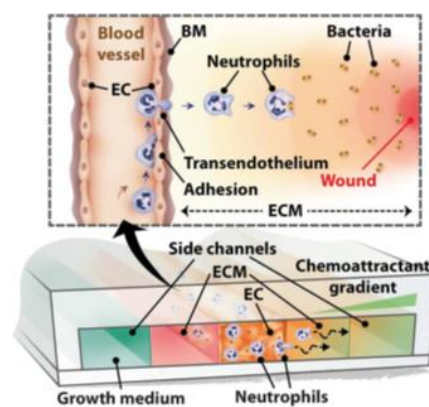


Figure 9 - Cross-sectional image of Han's microfluidic device in which are comprised: a medium channel on the left; an endothelial channel in the middle surrounded by two channels that include ECM components; a channel that comprise chemokine on the right [51].

Subsequent microfluidic devices considered also the influence of shear stress. Indeed, Jeon et al. studied extravasation of tumor cells during metastatic process in dynamic and static conditions by means of device that mimicked perfusable micro-vascularized bone micro-environment (Figure 10) [52]. Cancer cells extravasate in the gel into the bone-like micro-environment in response to a molecular gradient of chemoattractant factors produced naturally by osteo-differentiated cells. Although, it overcame the static limitation of previous devices, it does not have a tight monolayer of endothelial cell but a network, which is not suitable for study monocyte extravasation.

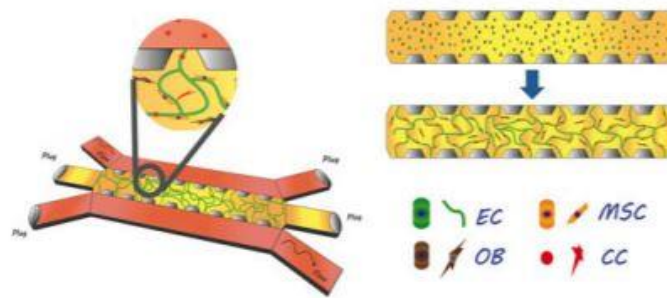


Figure 10 - Human 3D vascularized organotypic microfluidic assays to study breast cancer cell extravasation [52]

Recently, it was developed a new microfluidic device (Figure 11) that allows to assess the interdependent steps underlying leukocyte trafficking. This system is able to reproduce simultaneously all fundamental component of extravasation process, including controlled fluid condition, endothelial monolayer, 3D ECM and chemoattractant gradient. In particular, leukocytes flow over an endothelium coated filter under controlled shear stress by means of a syringe pump. These conditions allow to reproduce leukocyte TEM and performing real-time high-resolution imaging of these processes [53]. However, in this system was not included supporting cells and the ECM, thus it did not resemble completely the synovial joint.

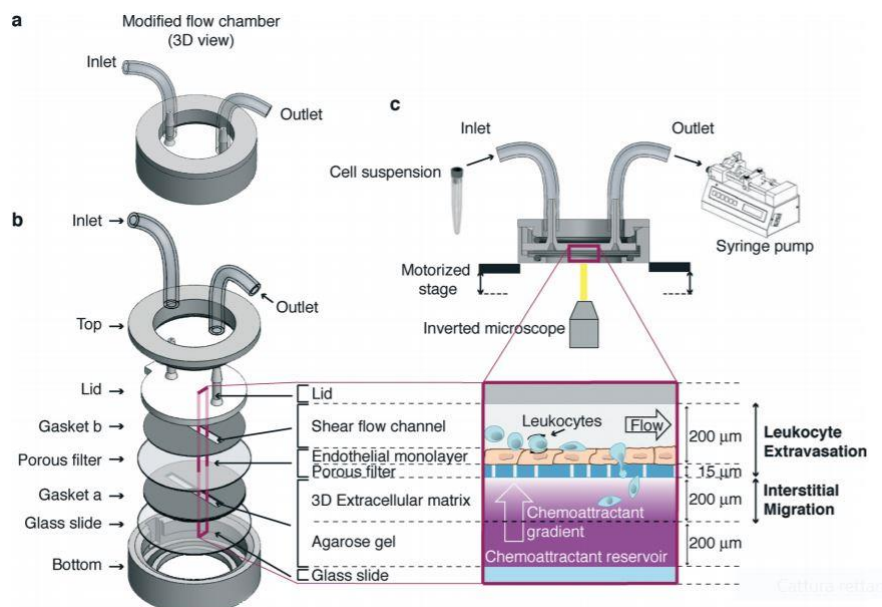


Figure 11 - Overview of the microfluidic device developed by Molteni et al. a) 3D representation of the device; b) schematic representation of the components present in the device; c) experimental set-up [53].

2. Aim of the thesis

OA is one of the most diffused joint disease affecting millions of people. The lack of specific treatments able to counteract disease progression and joint degeneration make OA a very debilitating disease. For this reason, a thorough investigation of the mechanisms and events leading to OA onset and progression must be pursued. In this context, the possibility to develop organotypic models that allow recapitulating *in vitro* the complexity of the *in vivo* situation is an invaluable opportunity, made possible by new fabrication technologies. Here, we propose an innovative microfluidic chip that is able to model the OA joint and specifically designed to model monocyte extravasation from a post-capillary venule to the adjacent synovial membrane following chemoattractant signals. Indeed, OA patients show an increased accumulation of monocytes/macrophages in the synovial membrane, caused by an abnormal recruitment of monocytes from the bloodstream.

The model mimics the synovial membrane with a post-capillary venule, a synovial fluid channel and the articular cartilage. In particular, a synovial compartment composed of synovial fibroblasts (SFb) embedded in fibrin hydrogel with an endothelialized channel reproduces the synovial membrane. Articular cartilage is resembled with an articular compartment composed of articular chondrocytes (ACh) embedded in fibrin hydrogel. Moreover, a channel for synovial fluid injection separates the synovial and cartilage compartments. Monocytes isolated from human blood samples of healthy donors are injected in the endothelialized channel and the extravasation is detected (Figure 12).

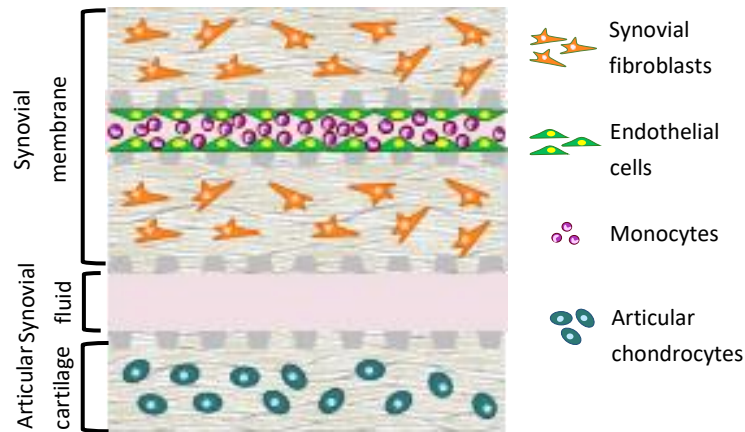


Figure 12 – Schematic representation of the device used in this project comprising all cell types used. From top to bottom: synovial membrane formed by synovial fibroblasts embedding a post-capillary venule formed by endothelial cells; synovial fluid channel resembling the joint cavity; articular cartilage formed by articular chondrocytes.

The aim of this thesis was the optimization of the biophysical and biochemical stimulation of the endothelial monolayer to approach the conditions that endothelial cells encounter *in vivo*, and the biological validation of this model testing monocyte extravasation in response to different chemoattractants. In particular, we tested the effect of shear stress and inflammation on the expression of adhesion molecules directly involved in monocyte extravasation. After selecting the best pre-conditioning treatment, the model was firstly validated evaluating monocyte extravasation towards a known chemokine mix. Subsequently, we assessed the chemoattractant effect of OA synovial fluid. Moreover, we inspected the role of tissue-specific cells (SFb and ACh), comparing monocyte extravasation in the complete system with the system without tissue-specific cells. After validating the model and proving that OA synovial fluid acts as a chemoattractant signal able to induce monocyte extravasation, we performed a preliminary investigation on the cytotoxicity of different antagonists for specific chemokine receptor on the endothelial cells, which are known to be very sensitive to culture conditions. The final aim of this project is indeed to use the developed model as a platform to screen the ability of different antagonists to occupy the chemokine receptors on monocytes in order to inhibit their extravasation. In this perspective, the cytotoxicity experiments performed will give indications about the antagonist concentrations that can be applied in the model without impairing endothelial cells viability. .

3. Materials and Methods

3.1. Fabrication of the microfluidic device

The aim of this thesis is to use a microfluidic organotypic device that resembles an osteoarthritic joint in order to study the monocyte extravasation process. The chip is a multi-channel microfluidic device, representing different compartments that are synovium with a post-capillary venule composed respectively of SFb and endothelial cells, and cartilage formed by ACh with a synovial fluid channel filling the gap between them.

The length and height of all channels are 10000 μm and 100 μm , respectively. The width of the post-capillary channel is 200 μm in order to resemble as much as possible the physiological dimension of a post-capillary venule and at the same time to guarantee the feasibility of the microfluidic device fabrication. The width of synovial membrane and cartilage compartments is 400 μm , which allows the injection of fibrin gel avoiding gel leakage in the adjacent compartments. Moreover, these dimensions guarantee a correct diffusion of chemokines throughout the device from the synovial fluid channel. Considering the high viscosity of synovial fluid, the width of the synovial fluid channel enables the injection of such a viscous fluid without applying much pressure and consequently, minimizing the chance of damaging the adjacent gel compartments. Channels are separated by a linear array of regularly spaced (90 μm) trapezoidal posts (or pillars), with bases and height measuring respectively 56 μm , 160 μm and 90 μm (Figure 13). The use of pillars allows confining the cell-laden hydrogel compartments, preventing gel leakage into the medium channels. Moreover, they enable cell migration, diffusion of molecules, nutrients and waste products of the cells.

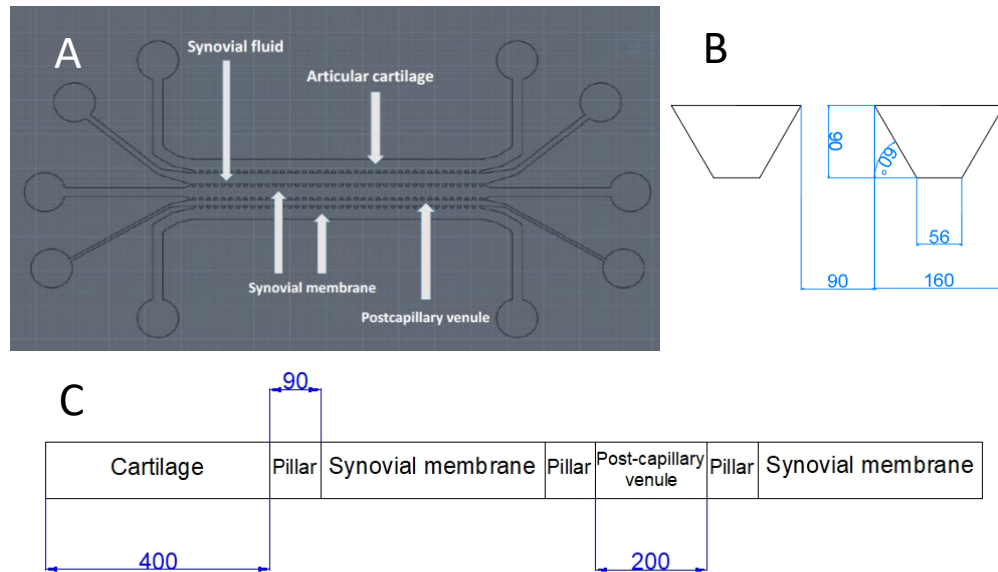


Figure 13 - (A) CAD representation of the microfluidic device for monocyte extravasation model; (B) Pillar specification, all dimensions are expressed in μm ; (C) Cross-sectional representation of the device, all dimensions are expressed in μm

The layout of the desired device was previously obtained by means of AUTOCAD software (Autodesk®) and printed at high resolution (64000 DPI) on a Mylar® polyester film. The obtained transparency mask was then used for the photolithography process to transfer the designed patterns on a SU-8 negative photoresist, creating a silicon wafer master. The master fabrication process was performed in the clean room of PoliFAB (micro and nano technology center, Politecnico di Milano) with controlled environment in terms of humidity, temperature and clean atmosphere without the presence of particulate. Specifically, the SU-8 photoresist was spin coated over the silicon wafer in order to have a uniform distribution with a height of 100 μm and the photomask was then placed on top of the SU-8 layer. After that, SU-8 was exposed to UV light. The parts that were not covered by the photomasks polymerized, while the unexposed parts were removed with a developer (organic solvent solution). Thus, the obtained master mold was used to produce the microfluidic devices by PDMS replica molding. However, before using the master, it was exposed to tri-methylchloro-silane (TMSC) for 15 minutes to ease the peeling off process of the PDMS from the wafer. The PDMS elastomer (Sylgard® 184) was mixed with the curing agent at ratio of 1:10 (1 part of curing agent for 10 parts of elastomer). After the two components were well mixed, the mixture was centrifuged at 500 g for 30 seconds to remove all the bubbles and

it was poured over the wafer. Finally, the wafer was degassed in a vacuum chamber for 30 minutes and left to polymerize ON. This long time impeded the PDMS to shrink excessively, obtaining a microfluidic device with the same dimensions as on the master. Then, the chips were detached from the silicon wafer by using a spatula, paying attention not to damage

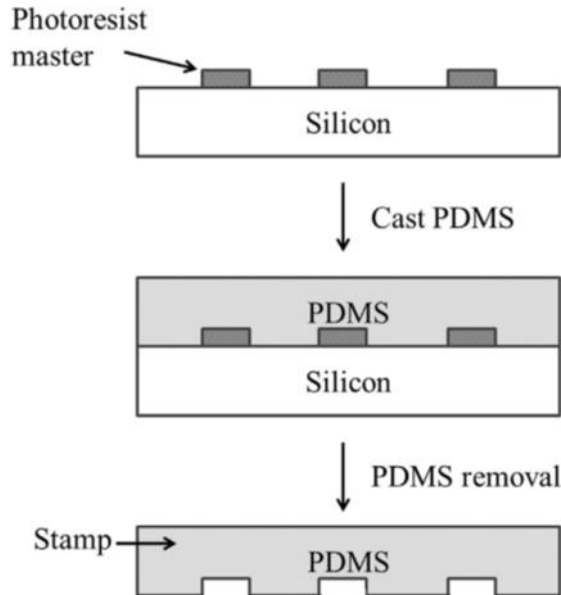


Figure 14 - Schematic representation of PDMS pouring, polymerization and detachment from the silicon wafer master

the silicon wafer (Figure 14).

Since the silicon wafer is very fragile, we used the PDMS chip obtained from the silicon wafer as a master mold to produce resins that were used for the replica molding process. To this purpose, component A and component B (Epoxy resin, C-System 10-10 CFS) of the resin were mixed in ratio 2:1, and then degassed in a vacuum chamber. Thus, the mixture was poured on the PDMS master mold with the features on the upper side and left to polymerize ON. After that, the master mold was removed and the resin was exposed to TMSC in order to ease the detachment of the PDMS chip from the resin. The resin molds were then used to produce the microfluidic chips using the same procedure as for the silicon wafer master.

To obtain the access ports for the gel injection and for the culture media channel, biopsy punchers were used. Specifically, a 1 mm-diameter puncher was used for all the inlets and for the outlets of the gel compartments, while a 4 mm-diameter puncher was used to make the reservoir of the endothelial and medium channel (Figure 15).

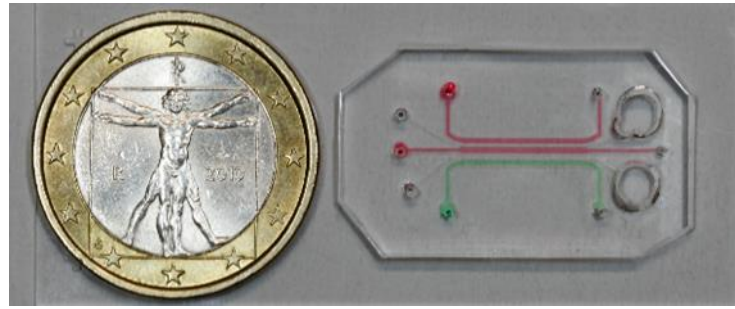


Figure 15 - Picture of the microfluidic device. The channels for SFb seeding are evidenced in red, while the channel for ACh seeding is shown in green.

In order to form the channels, the devices were subsequently bonded to a glass coverslip by plasma treatment. Briefly, the glasses were cleaned with acetone, isopropanol and milli-Q water, and dried using compressed air. Glasses and microfluidic chips with upwards features were placed in the plasma cleaner machine. After 1 minute of vacuum, samples were subjected to 1 minute of oxygen plasma treatment. Subsequently, the PDMS devices were bonded to the glass coverslips gently pressing to remove bubbles. In order to favor the bonding, the chips were placed on a hot plate at 100° C for 10 minutes. Afterwards, the devices were sterilized in autoclave and dried in the oven at 65°C for 9 hours. Then, the chips were ready to be used for the subsequent experiments.

3.2. Biological Validation

3.2.1. Cell isolation and culture

To perform the biological validation of the model, we used different cell types: synovial fibroblasts and articular chondrocytes to simulate respectively the synovial membrane and the articular cartilage, endothelial cells to reproduce a post-capillary venule inside the synovial membrane, and monocytes to perform the extravasation assay. More details regarding each cell type are described below.

3.2.1.1. Synovial fibroblast isolation

Synovial fibroblasts (SFb) were isolated from biopsies of synovial membrane obtained from OA patients that had undergone total knee replacement, after obtaining written informed consent. Synovial membrane was processed within two hours since receiving the tissue from the surgery room. The tissue was digested with 3 mg/mL Collagenase type I

(Worthington Biochemical Corporation) in serum-free DMEM (4500 mg/L D-glucose, Gibco) (4 mL of enzyme solution per tissue gram) in agitation at 37°C for 3 hours. The digestion was stopped by adding one volume of DMEM containing 10% of heat-inactivated Fetal Bovine Serum (FBS, Hyclone) and subsequently, the solution was filtered with a cell strainer (100 µm) to remove undigested tissue. After centrifuging the solution at 350 *g* for 5 minutes, the resulting cell pellet was suspended in 1 mL of complete medium (CM) composed of 10% FBS, 2 mM L-glutamine, 100 U/mL penicillin, 100 µg/mL streptomycin, 10 mM HEPES, 1 mM sodium pyruvate (all from Gibco) and counted under microscope with Burker chamber. Cells were seeded in culture flasks at density of 5000 cells/cm² and cultured under standard conditions (37°C, 5% CO₂) in CM. When sub-confluent, SFb were harvested and re-plated to keep them in exponential growing phase. Cells at second passage were harvested and frozen in 10% DMSO in FBS for subsequent experiments.

3.2.1.2. Articular chondrocyte isolation

Articular chondrocytes (ACh) were isolated from samples of articular cartilage obtained from OA patients that underwent total knee replacement surgery. Biological samples were obtained after written informed consent of patients. Articular cartilage was processed within two hours since receiving the tissue from the surgery room. After cutting the tissue in small pieces, articular cartilage was digested with 1.5 mg/mL Collagenase type II (Worthington Biochemical Corporation) in a mix of serum-free DMEM and CM (1:1, 10 mL of enzyme per tissue gram) for 22 hours at 37°C in agitation. After the digestion, the enzyme activity was stopped by adding one initial volume of CM. Then, the solution was filtered with a cell strainer (100 µm) to eliminate undigested tissue, and centrifuged at 350 *g* for 5 minutes. Cells were plated at density of 10000 cells/cm² and cultured under standard culture conditions (37°C, 5% CO₂) in CM supplemented with 0.5 mM L-proline (Sigma Aldrich) and 50 µg/mL L-ascorbic acid (Sigma Aldrich). When sub-confluent, ACh were harvested to keep them in exponential growing phase. Cells at second passage were harvested and frozen in 10% DMSO in FBS for subsequent experiments.

3.2.1.3. Thawing of SFb and ACh and culture

In order to limit the biological variability, we used a pool of cells isolated from three patients, both for SFb and ACh. After thawing, cells were centrifuged at 350 *g* for 5 minutes and suspended in fresh medium. Subsequently, cells were seeded in T75 flasks at a density of 6000 cell/cm². The day of the experiment, both SFb and ACh were washed once with Phosphate Buffer Solution (PBS) and detached by incubation with Trypsin-EDTA (0.05%, Gibco) for 5 minutes at 37°C. Enzyme activity was stopped by adding two volumes of CM. Then, SFb and ACh were counted and suspended at the desired concentration.

3.2.1.4. Endothelial cells

Endothelial cells were used to mimic the post-capillary venule presents in the synovial membrane. In particular, for our experiments we used Green Fluorescent Protein-Expressing Human Umbilical Vein Endothelial Cells (GFP-HUVECs). These cells constitutively express the fluorescent protein GFP, and emit green fluorescence when excited at the correct wavelength of light ($\lambda_{\text{excitation}} = 488 \text{ nm}$, $\lambda_{\text{emission}} = 507 \text{ nm}$). GFP-HUVECs were purchased from Angio-Proteomie at passage 3, expanded in Endothelial Growth Medium-2 (EGM-2, Lonza) until passage 6, and subsequently frozen in 10% DMSO in FBS until needed.

After thawing, cells were directly seeded in T25 flasks at a density of 20000 cell/cm² and cultured in EGM-2. The day of the experiment, GFP-HUVECs were washed once with PBS and harvested using Trypsin-EDTA (0.05%, Gibco) for 2 minutes at RT. After stopping the enzyme activity by adding EGM-2 medium, cells were collected, counted and suspended at the desired concentration.

3.2.1.5. Monocytes

Monocytes were isolated from the buffy-coats of healthy blood donors obtained from the local blood bank. Monocytes were positively selected from peripheral blood mononuclear cells (PBMCs) isolated using Ficoll-Hypaque (GE Healthcare) density gradient separation. Briefly, blood sample was diluted with PBS 1:1 and gently stratified over Ficoll-Hypaque at a ratio 2:1. Subsequently, tubes were centrifuged at 900 *g* for 30 minutes at 18°C. After

centrifuging, the blood was separated as shown in Figure 16 and PBMCs were stratified in the interface between the upper yellowish plasma layer and the lower Ficoll layer.

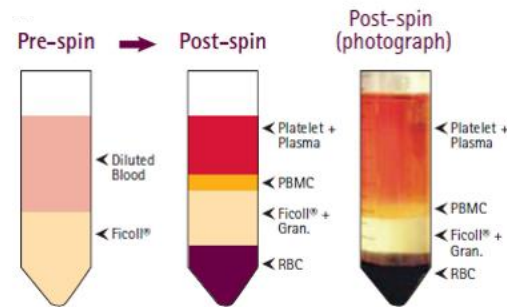


Figure 16 - PBMCs isolation by density gradient centrifugation using Ficoll-Hypaque. After centrifugation, PBMC were stratified between the upper plasma layer and the lower Ficoll layer, while red blood cells were stratified at the bottom of the falcon tube.

PBMCs were carefully collected using a pipette making sure to not collect the Ficoll phase, suspended in PBS and centrifuged at 760 *g* for 10 minutes at RT. To remove platelets, PBMCs were suspended in PBS and centrifuged at 200 *g* for 15 minutes at RT. Cells were subsequently suspended in 5 mL of FACS buffer (0.5 % Bovine Serum Albumin, Sigma Aldrich, 2 mM EDTA, Sigma Aldrich, in PBS) and counted.

Monocytes were positively isolated from PBMCs with CD14+ MicroBeads (Miltenyi Biotech), a solution of magnetic micro-beads conjugated to human monoclonal antibodies against CD14 antigen, which is strongly expressed by monocytes. After centrifuging the cell suspension at 300 *g* for 10 minutes, PBMCs were suspended in the CD14+ MicroBeads solution and incubated for 20 minutes at 4° C. Cells were washed once with FACS buffer and loaded into a MACS separation column to magnetically separate CD14+ cells. Labeled monocytes were retained in the magnetic MACS column immersed in a magnetic field, while the non-labeled cells passed through. Eluted positive cells were counted, centrifuged and suspended in RPMI (Gibco) added with 2% FBS, 2 mM L-glutamine, 100 U/mL penicillin, 100 µg/mL streptomycin at 1x10⁶ cells/mL.

In order to visualize cells during the extravasation assay, monocytes were stained with Vybrant™ cell-labeling solution DiD (Invitrogen), a highly lipophilic fluorescent dye that fluorescently stains the cytoplasmic membrane. Following the manufacturer's instructions, cell suspension was added with 2 µL/mL Vybrant™ solution and incubated at 37°C for 7

minutes. After two washing steps with fresh medium, cells were counted and suspended at concentration of 4 M/mL before the injection into the microfluidic device.

3.2.2. Synovial Fluid

The synovial fluid was processed immediately after collection from OA patients who had undergone total knee replacement after obtaining informed consent. The synovial fluid was centrifuged at 3000 *g* for 10 minutes at 4°C to remove possible erythrocytes and other debris, aliquoted and stored at -80°C for subsequent experiments.

3.2.3. Cell embedding in fibrin hydrogel

To perform the experiments for this project, SFb and ACh were embedded in fibrin hydrogels to simulate synovial membrane and articular cartilage in the respective channels of the microfluidic device. Cell density (2.5×10^6 cells/mL) and fibrin concentration (10 mg/mL) used in this thesis were previously defined in a preliminary work. SFb and ACh were cultured as described in section 3.2.1.3. For fibrin embedding, sub-confluent cells were harvested, counted and suspended in human thrombin (4 UI/mL diluted in 40 mM CaCl₂, Tisseel kit, Baxter) at a concentration of 5×10^6 cells/mL. The cell suspension was mixed 1:1 with human fibrinogen (20 mg/mL in PBS, Sigma-Aldrich) and quickly injected into the inlet of the corresponding compartment of the device. The chips were incubated at 37°C and 5% CO₂ for 5 minutes to let the gels polymerize. Subsequently, CM and a solution containing 5 µg/mL fibronectin (EMD Millipore) was injected in the synovial fluid channel and in the endothelial channel, respectively. Fibronectin is a glycoprotein of the extracellular matrix that binds to integrins present on cells, thus facilitating the adhesion of endothelial cells. Chips were placed in a humidified chamber in incubator for 1 hour.

3.2.4. Endothelial monolayer formation

To simulate in our device a synovial post-capillary venule, we used endothelial cells to generate an endothelial monolayer on the walls of the channel included in the synovial membrane compartment. The monolayer must be tight and cover all the length of the channel in order to have a separation of environments in the device.

After cell embedding in fibrin hydrogel and fibronectin coating, the endothelial channel was washed with EGM-2. Endothelial cells were harvested, counted and suspended at a concentration of 6×10^6 cells/mL in EGM-2 with 20% FBS. Afterwards, 10 μ L of cell suspension were placed in the reservoir of the endothelial channel and the chip was put slipping towards the inlet at 37° C for 15 minutes. Once endothelial cells covered all the channel, 50 μ L of EGM-2 with 10% FBS and 50 μ L of CM were added to reservoir of the endothelial channel and the synovial fluid channel respectively. Chips were cultured in incubator ON.

3.2.5. Endothelial cell pre-conditioning

In order to mimic the physiological conditions and the inflammation state that occur *in vivo*, endothelial cells seeded in the device were subjected to a pre-conditioning treatment. In particular, endothelial cells were activated by flow-induced shear stress and exposure to TNF- α . To select the optimal parameters, we performed immunofluorescent assays to detect the protein expression of ICAM-1 and VCAM-1 in endothelial cells either maintained in static conditions or subjected to different flow rates, combined with TNF- α or not.

The flow was applied by means of a syringe pump (PHD 2000, Harvard Apparatus). Chips were perfused either with EGM-2 or EGM-2 added with 2 ng/mL TNF- α , depending on the experimental group, for 3 hours. Chips maintained in static conditions were used as control samples. After 3 hours, chips were removed from the pump and the endothelial channels were washed with PBS, fixed with paraformaldehyde 2% in PBS (PFA, Santa Cruz Biotechnology) for 10 minutes at RT, washed with PBS and stored at 4° C until staining.

To block nonspecific antibody binding, the endothelial channel was incubated with a blocking solution containing 1% BSA in HBSS (Gibco) for 30 minutes at RT in slow agitation. Subsequently, the endothelial channel was incubated with the primary antibody (Ab) ON at 4°C in slow agitation. ICAM-1 and VCAM-1 were detected using a mouse monoclonal Ab (1:100, Santa Cruz) and a rabbit monoclonal Ab (1:200, Abcam), respectively. After washing with HBSS, chips were incubated 1 hour at 37°C in slow agitation in the dark with the secondary Ab. As secondary Abs, the Alexa Fluor® 647 goat anti-mouse IgG (1:1000, Invitrogen) and the Alexa Fluor® 647 goat anti-rabbit IgG (1:500, Invitrogen) were used to detect ICAM-1 and VCAM-1, respectively. After washing with HBBS, endothelial channels

were incubated 2 minutes at RT with the nuclear staining Syto82 (Invitrogen) diluted 1:2000 in HBSS. Chips were stored in the dark at 4°C until observation. Pictures of the specific signal on endothelial cells were taken with a confocal microscope (Leica SP8).

3.2.6. Model validation

To validate the developed model, we quantified the extravasation of primary human monocytes in response to a known chemokine mix composed of 50 ng/mL Macrophage Inflammatory Protein-1 α (MIP-1 α), 50 ng/mL Monocyte Chemoattractant Protein 1 (MCP-1), 50 ng/mL RANTES and 50 ng/mL Macrophage Inflammatory Proteins-1 β (MIP-1 β) in CM. CM with 2% FBS was used in control samples.

Chips were prepared as previously described and after endothelial cell pre-conditioning, endothelial and synovial fluid channels were washed with EGM-2 and CM respectively to remove the excess of TNF- α . Monocytes were isolated as described in section 3.2.1.4. Afterwards, 20 μ L of cell suspension were placed in the reservoir of endothelial channel. Chips were put slipping towards the inlet for 15 minutes to allow the cells to enter the channel and subsequently cultured in a humidified chamber ON. The day after, chips were observed at 10X magnification under a confocal microscope (Leica SP8). Pictures of the synovium compartment, which includes both synovial membrane channels and the endothelialized channel, were taken with a z-stack of 100 μ m in order to observe all the height of the device (z-step: 1 μ m).

3.2.7. Monocyte extravasation assay

To investigate the chemoattractant effect of synovial fluid on monocyte extravasation, we performed extravasation experiments analyzing the response to synovial fluid. Moreover, we tested the influence of tissue-specific cells (SFb and ACh) on the extravasation process. Therefore, microfluidic chips were prepared with either plain or cell-loaded fibrin hydrogels. To visualize the different cell populations inside the device, SFb and ACh were stained before gel embedding respectively with Vybrant™ Dil and Vybrant™ DiO cell-labeling solution (Invitrogen), following the manufacturer's instructions. All the samples were then seeded with endothelial cells and subjected to pre-conditioning or not, as previously described (see section 3.2.5). Immediately after isolation, monocytes were

injected in the endothelial channel. A mix of synovial fluids obtained from 3 OA patients was injected in the synovial fluid channel, while CM with 2% FBS was used as control. Chips were cultured in a humidified chamber ON. The day after, chips were observed at 5X magnification with a confocal microscope (Leica SP8). Pictures of the synovium compartment, which include both synovial membrane channels and the endothelialized channel, were taken with a z-stack of 100 μm in order to observe the entire height of the device (z-step of 2 μm).

3.2.8. Monocyte extravasation quantification

Analysis of the pictures taken with the confocal microscope were performed with ImageJ software. In particular, we used a macro script to automatize the process of analysis.

The macro script is reported below:

1. *path1=getDirectory("My output dir");*
2. *title = getTitle();*
3. *run("Split Channels");*
4. *run("Merge Channels...", "c2=[C1-" + title + "]" c6=[C3-" + title + "]"");*
5. *run("Z Project...", "projection=[Max Intensity]");*
6. *ztitle = getTitle();*
7. *waitForUser("Draw first ROI, then hit OK");*
8. *run("Duplicate...", "duplicate channels=2");*
9. *setAutoThreshold("Default dark");*
10. *//run("Threshold...");*
11. *call("ij.plugin.frame.ThresholdAdjuster.setMode", "B&W");*
12. *setThreshold(30, 255);*
13. *run("Convert to Mask");*
14. *run("Make Binary");*
15. *run("Watershed");*
16. *saveAs("Tiff", path1+title+"Ch_dx.tif");*
17. *run("Analyze Particles...", "size=20-100 show=Outlines clear summarize");*
18. *saveAs("Tiff", path1+title+"Outlines_Ch_dx.tif");*
19. *selectWindow(ztitle);*
20. *waitForUser("Draw the second ROI, then hit OK");*


```

21. run("Duplicate...", "duplicate channels=2");
22. setAutoThreshold("Default dark");
23. //run("Threshold...");
24. call("ij.plugin.frame.ThresholdAdjuster.setMode", "B&W");
25. setThreshold(30, 255);
26. run("Convert to Mask");
27. run("Make Binary");
28. run("Watershed");
29. saveAs("Tiff", path1+title+"Ch_sx.tif");
30. run("Analyze Particles...", "size=20-100 show=Outlines clear summarize");
31. saveAs("Tiff", path1+title+"Outlines_Ch_sx.tif");
32. selectWindow("Summary");
33. saveAs("Results", path1+title+"Results.xls");

```

This macro used a multichannel z-stack image acquired by a confocal microscope. The macro permits to split the detected channels, to merge them assigning a different color to each channel, and to form a z-projection with maximum intensity. We quantified the number of monocytes extravasated in the lower synovial compartment and in the upper synovial compartment. Therefore, for each compartment the script analyzes a region of interest (ROI) and applies a threshold (min = 30 and max = 255) in order to remove the background. Afterwards, the image is converted into a binary image and the watershed tool is applied, in order to separate close cells. Finally, the macro uses the analyze particle tool to quantify the extravasated monocytes with a range size comprised between 20-100 μm^2 . The script returns as an output the processed image and a numerical table comprising the number of extravasated monocytes for both ROI.

3.2.9. Statistical analysis

Different regions of the same chip were mediated and used as single data. Independent experiments were performed using monocytes from independent blood donors. Specifically, validation experiments with chemokines were conducted using monocytes from 5 different donors, while experiments with synovial fluid were conducted using monocytes from 7 different blood donors. To reduce biological variability, we used pools

of synovial fibroblasts, articular chondrocytes, and synovial fluid, each obtained from 3 OA donors.

Statistical analyses regarding monocyte extravasation were made by GraphPad Prism software (GraphPad Software). To evaluate the statistical significance of differences in monocyte extravasation between the upper and lower synovial compartment, it was applied a Student's t-test. Moreover, Student's t-test was used to evaluate the statistical significance between extravasation in the lower compartment in the control group and the chemokine mix or between the control group and the synovial fluid mix. Furthermore, a Two-Way ANOVA was used to analyze the influence of the preconditioning treatment on endothelial cells and of supporting cells on monocyte extravasation.

3.3. Cytotoxicity assay

3.3.1. Experimental design and procedure

After the device was validated to mimic monocyte extravasation in OA synovial joint, the further step will be to use the same device to test drugs with the aim of inhibiting monocyte extravasation and potentially reduce joint inflammation. In particular, we will focus on the use of antagonists of chemokine receptors present on the surface of monocytes. Since HUVECs are very sensitive to culture conditions, we performed a preliminary assay to evaluate the cytotoxicity of the following antagonists: BX 471 (CCR1-antagonist), RS 504393 (CCR2-antagonist), SB 328437 (CCR3-antagonist), AZD 2098 (CCR4-antagonist), Maraviroc (CCR5-antagonist) and Cenicriviroc (CVC) which inhibits both CCR2 and CCR5 [54] (all from Tocris). Furthermore, we evaluated the cytotoxicity of all the antagonists combined together (excluding CVC).

Cytotoxicity assay was performed in 96 multi-well plate on endothelial cells subjected to a treatment similar to endothelial monolayer in the device. Briefly, endothelial cells were seeded at 3125 cells/cm² in each well. After 24 hours, the medium was replaced with EGM-2 + 2 ng/mL TNF- α or EGM-2 alone based on the corresponding experimental group. After 3 hours, the medium was replaced with medium containing each specific antagonist or the antagonist combination at 1 μ M or 10 μ M. Considering that EGM-2 is rich of growth factors that promote endothelial cells viability and proliferation, we tested the antagonists both dissolved in RPMI-based medium (i.e. the optimal medium for monocytes used in the

extravasation experiments) and in a mix of RPMI and EGM-2 media (50:50). The next day, cell viability was analyzed by Alamar Blue assay (Invitrogen). This reagent contains resazurin, which is non-toxic, cell permeable and non-fluorescent. Once internalized by living cells, it is transformed in resorufin, which is a red colored and highly fluorescent compound that can be detected by fluorescence-plate readers allowing to quantify cell viability. Alamar Blue solution was prepared following the manufacturer's instruction, added to each well and incubated for 4 hours (37° C, 5% CO₂). Medium was then collected and transferred in black 96 multi-well plates to detect fluorescence at 450 nm using a plate reader (Victor X3, Perkin Elmer).

4. Results

4.1. Biological validation

4.1.1. Description of the microfluidic device

The main aim of this thesis was to validate a microfluidic device that mimics an OA joint. In particular, this device is employed to study the extravasation of monocytes from a post-capillary venule toward the synovial membrane in response to a chemoattractant stimulus. Parameters for embedding SFb and ACh in fibrin hydrogel and correct endothelial monolayer formation had been previously optimized. These results allowed us to obtain a device that comprised a cartilage compartment and a synovial membrane compartment embedding a narrow post-capillary venule in which monocytes are injected. Figure 17 shows all the cell types used to reproduce the extravasation process in the OA joint. In particular, we used SFb and ACh to mimic respectively the synovial membrane and the articular cartilage, and endothelial cells to resemble the post-capillary venule. Moreover, we used freshly isolated monocytes to perform the extravasation assay.

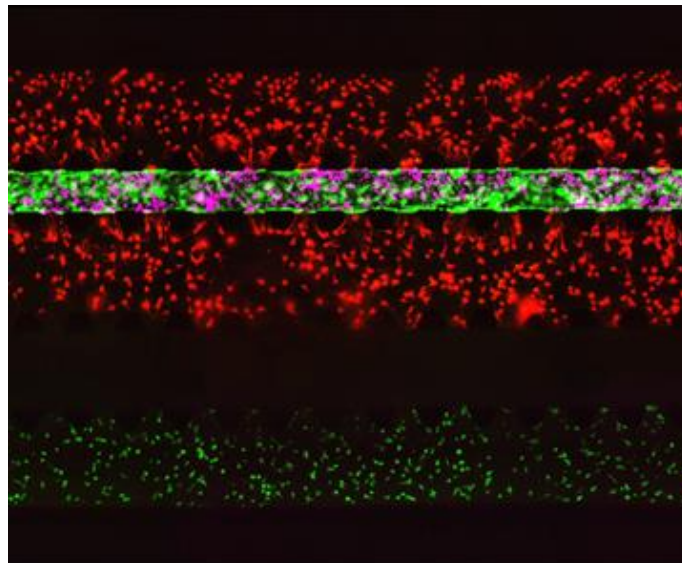


Figure 17 – Picture showing all the types of cells used in our microfluidic chip. From top to bottom, in red synovial fibroblasts, in green HUVECs, in magenta monocytes and in green chondrocytes.

4.1.2. Expression of adhesion molecules

Before validating the model, we evaluated how the expression of adhesion molecules is influenced by the application of a shear stress on endothelial cells. Adhesion molecules are fundamental in monocyte recruitment because they allow monocytes to adhere firmly on the endothelial monolayer and guide them during the extravasation process. Since their expression is known to be deeply influenced by shear stress, we investigated the expression of ICAM-1 and VCAM-1 in endothelial cells maintained in static condition or subjected to different flow rates (5 $\mu\text{L/h}$, 10 $\mu\text{L/h}$, 15 $\mu\text{L/h}$ and 30 $\mu\text{L/h}$).

Once the endothelial monolayer was formed, chips were connected to the syringe pump or maintained in static condition for 3 hours. The expression of ICAM-1 was stimulated by the flow compared to the static control, with a positive correlation with the levels of shear stress. Indeed, the number of positive cells increased as the flow rate increased. Conversely, almost no endothelial cells in static condition expressed ICAM-1. On the other hand, in general, VCAM-1 was expressed at low levels and seemed to decrease with the increase in flow rate compared to the static control (Figure 18).

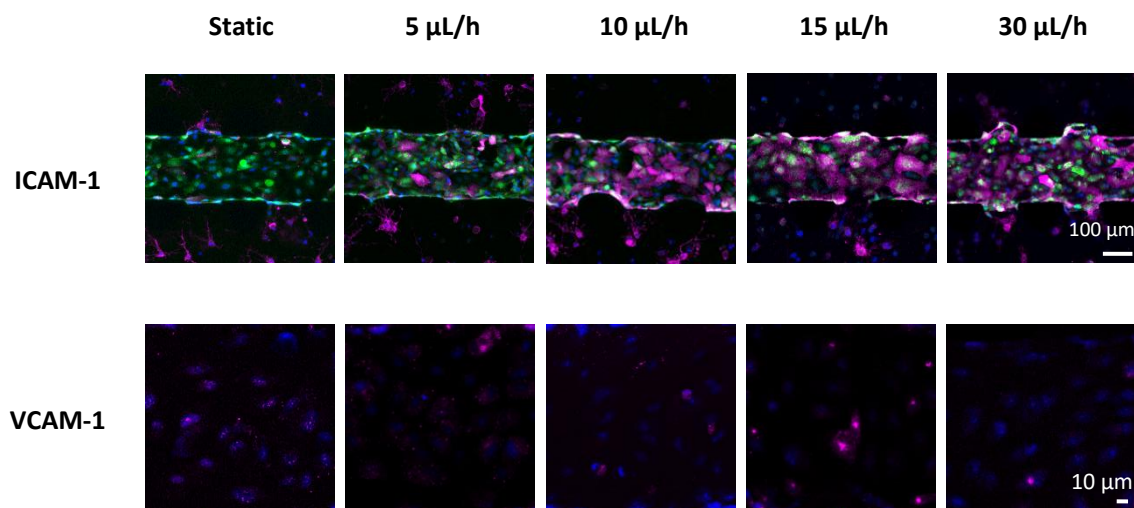


Figure 18 - Pictures showing the immuno-detection of ICAM-1 (first row) and VCAM-1 (second row) on endothelial cells subjected to perfusion at different flow rates (5 $\mu\text{L/h}$, 10 $\mu\text{L/h}$, 15 $\mu\text{L/h}$, 30 $\mu\text{L/h}$) or maintained in static condition. The specific signal of ICAM-1 and VCAM-1 is shown in magenta, endothelial cells in green and nuclei in blue. Pictures representing VCAM-1 are presented without the green signal of the endothelial cells, since it would hide the magenta signal specific of VCAM-1.

To test also the effect of inflammation on the expression of adhesion molecules, we selected the two conditions in which these proteins were most expressed (i.e. static condition for VCAM-1 and flow at 30 $\mu\text{L/h}$ for ICAM-1). Therefore, we evaluated the expression of ICAM-1 and VCAM-1 in response to TNF- α alone or combined with shear stress raised by flow at 30 $\mu\text{L/h}$. In the presence of TNF- α , the expression of both adhesion molecules was upregulated compared to that observed in endothelial cells that were not treated with TNF- α . In particular, TNF- α stimulated the expression of ICAM-1 more in dynamic (30 $\mu\text{L/h}$) than in static condition, suggesting a synergic effect of flow and TNF- α . On the other hand, VCAM-1 was upregulated in the presence of TNF- α more in static condition than in samples subjected to dynamic condition. However, TNF- α appeared as able to rescue the loss of VCAM-1 expression induced by fluid flow. Given these results, for the subsequent experiments, endothelial monolayer was pre-conditioned with fluid flow at 30 $\mu\text{L/h}$ and TNF- α (Figure 19) to mimic, at least partly, the conditions of shear stress experienced by endothelial cells and the inflammation-related signals to which synovial endothelial cells resident in an inflamed joint are subjected *in vivo*.

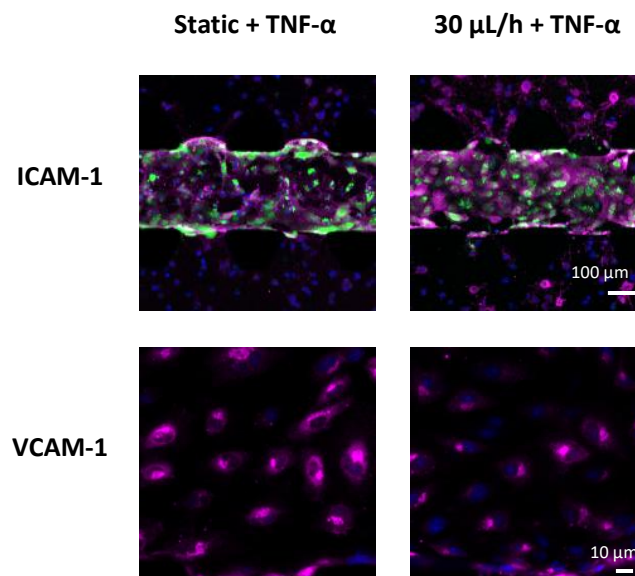


Figure 19 - Pictures showing the expression of ICAM-1 and VCAM-1 in endothelial cells subjected to TNF- α alone or combined with perfusion at 30 $\mu\text{L/h}$. Specific signal of adhesion proteins is represented in magenta, endothelial cells in green and nuclei in blue. Pictures representing VCAM-1 are presented without the green signal of the endothelial cells, since it would hide the magenta signal specific of the antibody.

4.1.3. Model validation

Once established the best parameters to pre-condition the endothelial cells, we performed the experiments to validate the model. Therefore, we evaluated the extravasation of monocytes in response to a chemokine mix of known composition compared to control groups without the chemokine mix.

After SFb and ACh injection in their respective channels in the device, we proceeded with endothelialization of the post-capillary venule channel as previously described. Subsequently, chips were pre-conditioned for 3 hours with perfusion at 30 $\mu\text{L/h}$ with TNF- α or maintained in static condition without TNF- α to assess the effect of the endothelial pre-conditioning on monocyte extravasation. After isolation and staining, monocytes were injected in the endothelialized channel of all devices. In the synovial fluid channel, either the chemokine mix or control medium was injected.

As shown in Figure 20, monocyte extravasation occurred only in the presence of the chemokine mix, while in the devices with control medium, monocytes remained confined in the endothelial channel, as evidenced also by the subsequent quantification obtained after picture analysis. In all the tested conditions, the analysis showed that monocytes extravasated specifically towards the chemokine mix in the lower synovial compartment instead of the upper compartment, confirming our hypothesis of specific extravasation. Moreover, the extravasation of monocytes was higher in samples with pre-conditioned endothelial cells than in samples without pre-conditioning, suggesting the importance of

treating endothelial cells with perfusion and inflammatory stimuli to resemble the *in vivo* process.

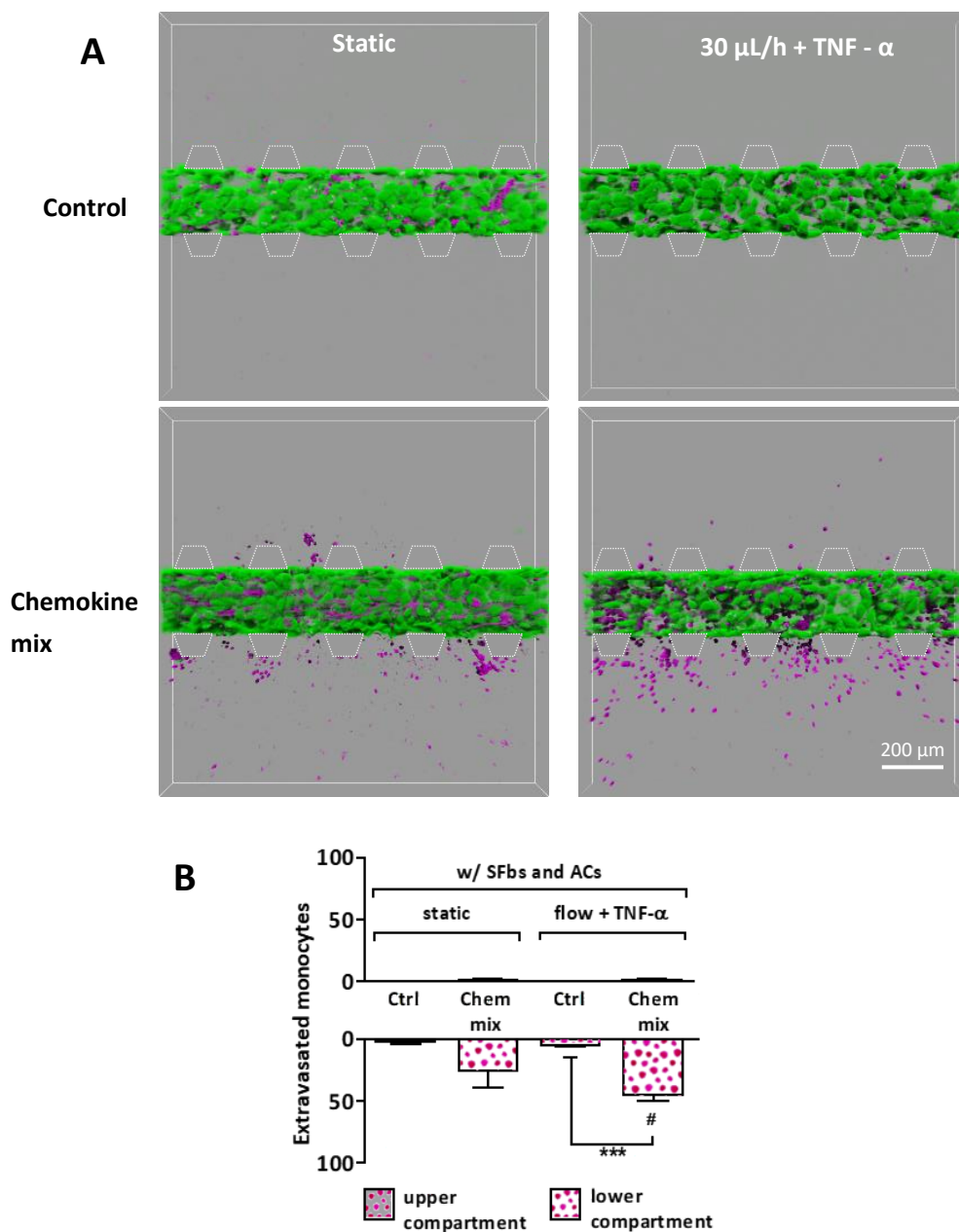


Figure 20 - A) 3D reconstruction of confocal pictures showing monocyte extravasation in response to control medium (upper row) or chemokine mix (lower row). Extravasation was evaluated in chip pre-conditioned with perfusion at 30 $\mu\text{L}/\text{h}$ combined with TNF- α (right column) and compared to a control group maintained in static (left column); B) Quantification of data obtained from picture analysis with our automated macro to count the number of extravasated monocytes in the upper and lower compartment in all the tested conditions.

4.1.4. Monocyte extravasation assay

After validating the model, we evaluated monocyte extravasation in the presence of synovial fluids obtained from OA patients using control medium as a comparison. Additionally, we compared the extravasation in the complete system with that occurring in the system in the absence of the supporting cells (SFb and ACh), in order to assess their influence on monocyte extravasation compared to an easier model without tissue-specific cells.

The devices were set up as previously described and maintained in static condition or treated with perfusion at 30 $\mu\text{L}/\text{h}$ and TNF- α to confirm the influence of the pre-conditioning. As shown in Figure 21, monocytes in the presence of control medium remained confined inside the endothelial channel, while they extravasated in the presence of synovial fluid, indicating the chemoattractant effect of OA synovial fluid. The directional extravasation towards the lower compartment induced by synovial fluid was significantly higher compared to the non-specific extravasation towards the upper compartment in all the tested conditions. Picture analysis showed a significant difference between extravasation in response to synovial fluid and to control medium in all the conditions. Surprisingly, a higher number of monocytes extravasated in the system without supporting cells (SFb and ACh) compared to the complete system. This result suggested that SFb and ACh have an important role in the extravasation process, and that the incorporation of tissue-specific cells allows mimicking *in vivo* conditions better than a simplified model. We hypothesized that supporting cells interacted and sequestered chemokines, resulting in a lower extravasation. In the end, coherently with the results obtained in the model validation, the pre-conditioning treatment with perfusion and TNF- α proved to greatly affect the extravasation of monocytes.

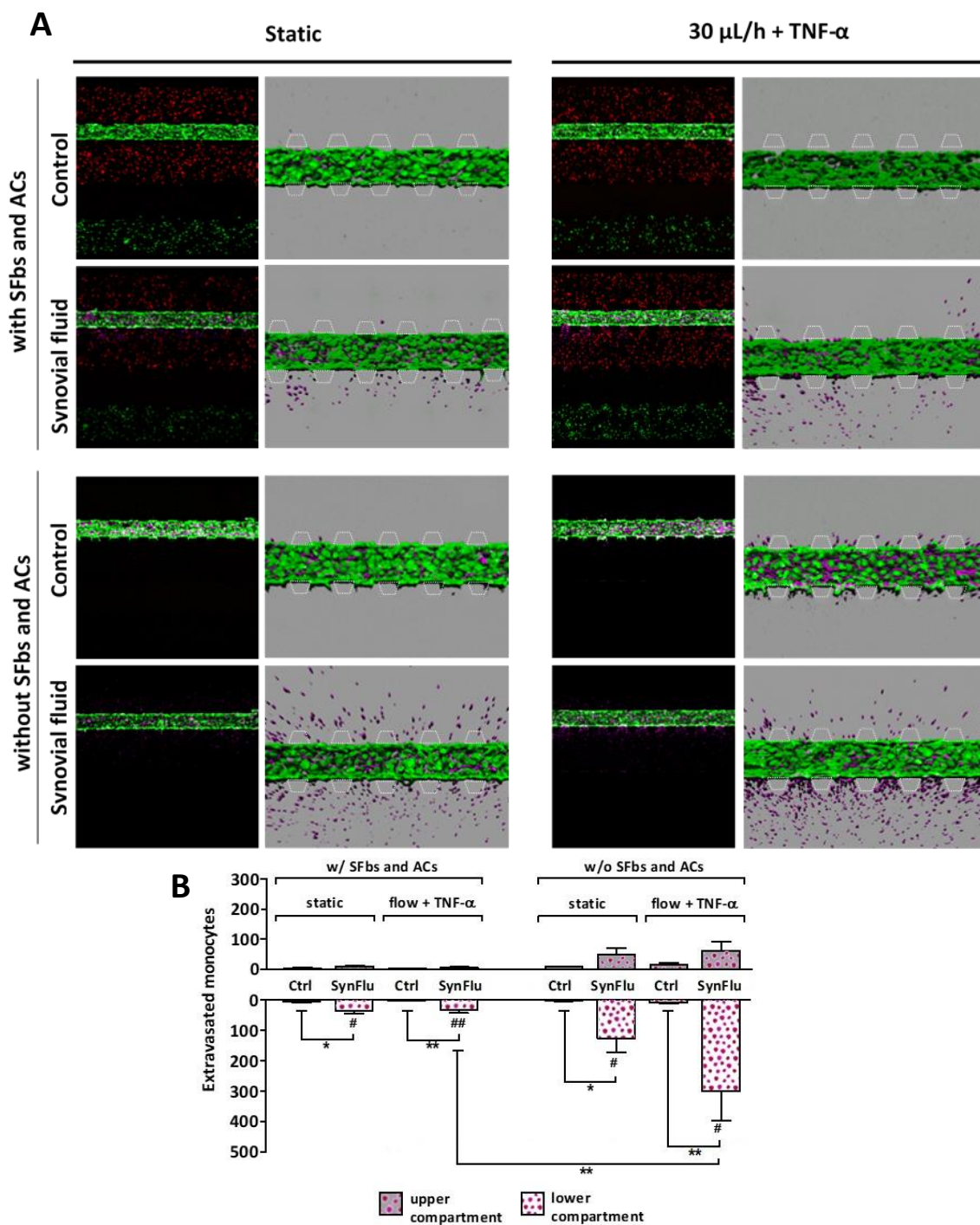


Figure 21 - A) Pictures showing monocyte extravasation in response to synovial fluid from OA patients (SynFlu) under static conditions (left column) or after perfusion with flow rate of 30 μ L/h combined with TNF- α (right column) compared to control group without synovial fluid (Ctrl). Extravasation was analyzed in complete systems or in devices without supporting cells. Black pictures highlight the presence or the absence of supporting cells in the different conditions (SFb are shown in red in the synovial compartment and ACh in green in the cartilage compartment). 3D reconstructions highlight the extravasated monocytes in magenta. B) Quantification of specific (lower compartment) and non-specific (upper compartment) monocyte extravasation in all the tested conditions.

4.2. Cytotoxicity assay

After proving that our model is a good tool to analyze the extravasation of monocytes in the presence of OA synovial fluid, the final goal of this project will be to use it to test the ability of different molecules to inhibit the extravasation process as a novel therapeutic strategy to counteract OA development. The idea was to use antagonists for chemokine receptors present on monocyte surface to prevent their binding to chemokines captured and exposed by endothelial cells on the luminal side of the vessel. Since endothelial cells are very sensitive to culture conditions, we decided to evaluate preliminarily the cytotoxicity of selected antagonists on endothelial cells. In particular, we used antagonists for CCR1, CCR2, CCR3, CCR4, CCR5 and CVC. CVC antagonist is able to interact with both CCR2 and CCR5, which are considered as the two major receptors involved in monocyte extravasation. Furthermore, we evaluated the cytotoxicity of all the antagonists combined together (excluding CVC), since inhibiting simultaneously all the considered receptors could be more effective than using single antagonists.

As shown in Figure 22, all the antagonists had a cytotoxic effect on endothelial cells that decreased at the lowest concentration (1 μM). Unexpectedly, the antagonists combined together had a similar or lower cytotoxic effect compared to single antagonists.

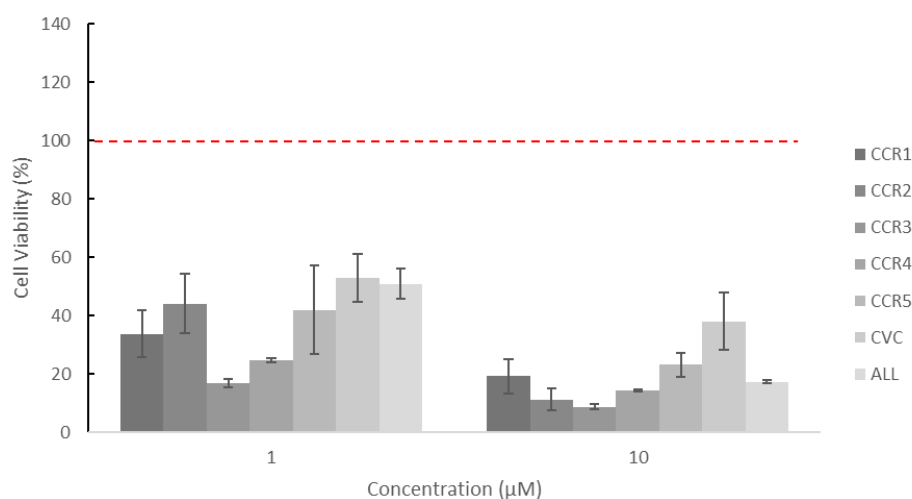


Figure 22 - Endothelial cell viability in response to chemokine receptor antagonists suspended in RPMI (at two different concentrations compared to the control group without antagonists (red dashed line)).

Since the purpose is to use the antagonists in our device, we also evaluated their cytotoxicity after treating endothelial cells with TNF- α for 3 hours, as in our chip. Control groups were treated with TNF- α in the corresponding medium without antagonists. Figure 23 shows that overall the antagonists had some cytotoxic effect. As expected, the cytotoxicity on endothelial cells was lower for the lowest antagonist concentration used. The combination of all the antagonists together resulted less or equally cytotoxic to that of single antagonists, confirming the previous results. Moreover, our results confirmed that TNF- α did not increase the cytotoxicity of the antagonists, suggesting that they do not have a synergic effect.

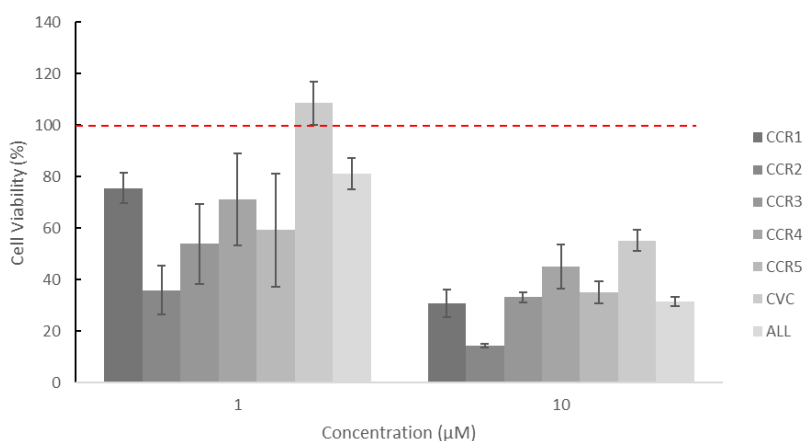


Figure 23 - Quantification of HUVECs viability in response to chemokine receptors' antagonists suspended in RPMI or in RPMI + EGM-2 at two different concentrations after endothelial cells have been preconditioned with TNF- α compared to the control group without antagonists but equally treated with TNF- α (red dashed line).

5. Discussion

OA is one of the most common joint disorders and is characterized by joint pain and loss of function. Many risk factors are associated with this pathology, including age and obesity. Contrary to the simple vision of the past that considered OA as a mere cartilage pathology, nowadays OA is regarded as a whole joint disease that affects all joint tissues [7]. Indeed, OA includes the loss of articular cartilage, pathological changes in the synovial tissue, subchondral bone thickening and osteophyte formation. Moreover, it presents an important inflammatory component [55]. Recently, it has been demonstrated the crucial role of the inflammation of synovial membrane (synovitis), characterized by the abnormal accumulation of monocytes/macrophages, which secrete pro-inflammatory cytokines, thus propagating the inflammatory process and contributing to OA progression [56]. Pro-inflammatory cytokines are indeed considered as main players involved in OA progression and are found at high level in synovial tissue, articular cartilage and subchondral bone of OA patients. Among these, TNF- α plays a major role, since it suppresses the synthesis of type II collagen from chondrocytes and induces the production of MMPs, promoting cartilage degradation. Moreover, TNF- α amplifies the pathology by inducing the release of other pro-inflammatory cytokines and chemokines from chondrocytes [10].

Currently, there are no effective therapies that can counteract or slow down the progression of OA. Present treatments based on nonsteroidal anti-inflammatory drugs (NSAID) can only alleviate the symptoms and, eventually, patients must undergo partial or total joint replacement. Recently, new therapeutic molecules, called DMOADs, have been developed to act directly on OA causes. DMOADs can target subchondral bone by inhibiting osteolytic proteases produced by osteoclasts, cartilage through the inhibition of MMPs or inflammation, thus stopping the progression of pathology, alleviating the symptoms and improving the tissue functions [11] Albeit these innovative therapies are promising, up to now they have proved unsuccessful results, as they showed to provoke side effects or the results were not different from control groups [12]. For these reasons, there is a great necessity to develop new drugs with novel targets.

Considering the role of inflammation during OA progression, a very recent concept in the development of advanced therapies is the possibility to interfere with monocyte

extravasation and prevent their accumulation in the synovial membrane [57]. To reach this objective, it is necessary to have a detailed knowledge of the mechanisms underlying monocyte extravasation.

Several systems have been developed to study the process of cell extravasation. For instance, macroscale systems, such as those based on modified versions of the Boyden chamber, have been applied in different fields to study the extravasation of leukocytes and metastatic cells. However, these systems, which are mostly static, have several intrinsic limitations such as the impossibility of reproducing a 3D physiological environment and the high influence of gravity on cell extravasation [51]. In this context, microfluidics is emerging as a novel technology that allows overcoming the above-mentioned disadvantages of macroscale systems. In addition, microfluidics has several benefits, such as reduced volume of reagents and samples, precise control of the microenvironment and the possibility to co-culture different cell types inside compartmentalized 3D matrices within the same device [53]. Due to these features, microfluidics permits to mimic complex anatomical units, such as the articular joint. Many microfluidic devices have been developed to study the extravasation of leukocytes, but most of them lack to consider the effect of shear stress and the presence of tissue-specific supporting cells [51][53]. However, so far, no microfluidic model has been designed either to specifically study the extravasation of monocytes in an inflamed environment or to recapitulate the tissue composition of the articular joint.

The main aim of this thesis was to validate a novel organotypic microfluidic device developed to investigate monocyte extravasation in the context of the OA joint. The device is constituted by different compartments, resembling specific components of the synovial joint. In particular, synovial fibroblasts, articular chondrocytes and endothelial cells are co-cultured to mimic respectively the vascularized synovial membrane and the articular cartilage. Endothelial cells are used to line a channel that mimics a synovial postcapillary venule where monocytes are injected to monitor their extravasation.

Leukocyte extravasation towards inflamed tissues involves multiple factors, such as the presence of chemoattractant signals and the phenotype of endothelial cells. The shear stress to which endothelial cells are physiologically subjected influences their phenotype

inducing cytoskeletal changing, and modifying cell morphology and gene expression. In particular, mechanical forces exerted by fluid flow directly modulate the expression of adhesion molecules mediating the adhesion of circulating cells to the endothelium, which is a key step in the extravasation process. For this reason, we focused on the expression of ICAM-1 and VCAM-1, two adhesion proteins with a main role in monocyte extravasation. Fluid flow experiments showed that in static conditions the expression of ICAM-1 was almost absent. On the other hand, the number of endothelial cells expressing ICAM-1 increased with increasing flow rates closer to physiological values. These results are in accordance with previous results demonstrating that the laminar flow upregulates the expression of ICAM-1 in endothelial cells [58]. On the contrary, VCAM-1 is differently regulated. Indeed, in our system it was more expressed in static or at low flow rates conditions than at higher shear stresses. Also this result is in line with previous literature indicating that VCAM-1 is downregulated by shear stress [59], suggesting that *in vivo* this molecule mediates leukocyte adhesion in regions subjected to lower shear stress levels. Afterwards, we combined the physical stimulus provided by the shear stress with a biochemical stimulus to treat the endothelial monolayer in order to model more accurately the *in vivo* situation. Indeed, recent studies showed that inflamed synovium presents high levels of pro-inflammatory cytokines [49, 60], amongst which TNF- α is the major one. TNF- α is known to interact with endothelial cells and mediate the inflammatory response, inducing the upregulation of both ICAM-1 and VCAM-1 [61]. Indeed, our results showed that TNF- α enhanced the expression of these adhesion molecules both in static and under flow conditions. ICAM-1 resulted more expressed by the combination of the two stimuli compared to TNF- α alone, suggesting a synergic effect. On the contrary, the expression of VCAM-1 slightly decreased when TNF- α was combined with flow compared to static condition. These results are in agreement with previous studies showing the interaction of TNF- α with shear stress on the expression of adhesion molecules, resulting in the upregulation of ICAM-1 by the presence of both factors, while VCAM-1 is highly upregulated by TNF- α and downregulated by shear stress [62].

Once we selected the optimal inflammatory and shear stress stimuli for endothelial cell preconditioning, to validate the model, we evaluated monocyte extravasation in response

to a chemoattractant mix, compared to a control group without chemoattractant stimulus. We used a chemokine mix (MCP-1, MIP-1 α , MIP-1 β , RANTES) known to attract monocytes [63]. Our experiments showed that monocytes extravasated exclusively in presence of the chemokine mix and migrated especially toward the synovial fluid compartment, indicating the specificity of the extravasation as directed by chemokine signaling. In addition, we verified that preconditioning played a key the extravasation process, indicating the need to resemble as closely as possible the *in vivo* condition. Indeed, a significant difference was observed between the control group and the chemokine mix only in the preconditioned systems. This evidence confirmed the previous findings on the expression of adhesion molecules after endothelium preconditioning, highlighting that an increase expression of ICAM-1 and VCAM-1 leads to a major recruitment of monocytes.

Subsequently, we investigated monocyte extravasation in response to OA synovial fluid compared to control group, to demonstrate that synovial fluid exerts a chemoattractant influence during OA pathogenesis. Several studies demonstrated the presence of cytokine and chemokines in the synovial fluid [25, 64]. In particular, synovial fibroblasts produce cytokines, such as TNF- α and IL-1 β , which in turn induce the expression of cytokines by all the joint-resident cells, leading to chronic inflammation [10]. This highlights the importance of having a model that includes also these cell types to achieve a system able to mimic the OA environment. Based on this premise, we investigated whether the presence of synovial fibroblasts and articular chondrocytes could influence monocyte extravasation. The results confirmed the chemoattractant influence of synovial fluid. Indeed, monocyte extravasation occurred only in the presence of synovial fluid in all the tested conditions. Moreover, extravasation appeared to be higher in the absence of tissue-specific cells compared to the complete system including both synovial fibroblasts and articular chondrocytes. We hypothesized that supporting cells interact with the chemokines sequestering them and reducing their local concentration. In this way, a lower amount of chemokines can reach the endothelial monolayer and be displayed to monocytes, which leads to a reduced extravasation. This hypothesis is supported by evidences showing the presence of chemokine receptors on fibroblasts of different tissues, when they are in the presence of inflammatory conditions [65]. Even though we do not know the specific interactions that

have brought us to this unexpected result, it is possible to state that synovial fibroblasts and articular chondrocytes play an important role in this process and therefore it is necessary to include them in the model to resemble more closely the OA joint.

The final aim for this model will be to be applied to test new anti-chemokine strategies and evaluate their effect on monocyte extravasation. In this perspective, we performed a preliminary investigation on the cytotoxicity of different antagonists of chemokine receptors on endothelial cells. The results showed that the selected antagonists exert a concentration-dependent cytotoxic effect on endothelial cells. The double antagonist targeting CCR2 and CCR5, Cenicriviroc (CVC), that is a highly promising compound since it targets simultaneously two key chemokine receptors, appeared as less cytotoxic compared to the other single antagonist, in line with pre-clinical and clinical studies where it was shown to have a low cytotoxicity [54, 66]. To resemble the treatment to which HUVECs are subjected in our model, we assessed the effect of the antagonists combined with preconditioning of endothelial cells with TNF- α . Surprisingly, cell viability was increased compared to cells that had not been treated with TNF- α . We hypothesized that TNF- α acts on endothelial cells not only increasing the expression of adhesion molecules, but also improving cell viability by activating the NF κ B pathway, in line with previous literature data [67].

6. Conclusion and future perspectives

In the present thesis, we validated a microfluidic organotypic model that recapitulates the process of monocyte extravasation in the context of the osteoarthritic joint. After selecting a strategy to precondition endothelial cells, we validated the model by proving the specific extravasation of monocytes in response to a known chemokine mix and demonstrated the importance of correctly stimulate the system to resemble *in vivo* processes. Moreover, we provided the first direct evidence of the chemoattractant effect of OA synovial fluid, which is able not only to guide monocyte migration but also to induce their extravasation from vessels. Finally, we demonstrated the importance to have a complete system that includes tissue-specific cell types for a more accurate resembling of the *in vivo* condition, showing that complex biological processes cannot be properly studied in oversimplified systems.

In the future, this chip will be used to study monocyte extravasation in patient-specific models, in order to test if different categories of patients have different extravasation rates. Moreover, the device will be used as a suitable platform to study the effect of potential OA drugs targeting the extravasation process, such as the antagonists for chemokine receptors on monocytes that we proposed in the last part of this study..

7. Bibliography

- [1] S. Glyn-Jones, A. J. Palmer, R. Agricola, A. J. Price, T. L. Vincent, H. Weinans e A. J. Carr, «Osteoarthritis,» *The Lancet*, vol. 386, n. 9991, pp. 376-387, 2015.
- [2] Y. Zhang e J. M. Jordan, *Epidemiology of osteoarthritis*, vol. 26, 2010, pp. 355-369.
- [3] T. M. Griffin e F. Guilak, «Why is obesity associated with osteoarthritis? Insights from mouse models of obesity,» *Biorheology*, vol. 45, n. 3-4, pp. 387-398, 2008.
- [4] R. C. Lawrence, ; Discussants, P. A. Dieppe, R. Hirsch, C. G. Helmick, J. M. Jordan, R. S. Kington, N. E. Lane, M. C. Nevitt, Y. Zhang, M. Sowers, T. Mcalindon, T. D. Spector, ; A. R. Poole, S. Z. Yanovski, G. Ateshian, L. Sharma, J. A. Buckwalter, K. D. Brandt, J. F. Fries e D. T. Felson, «Osteoarthritis: New Insights Part 1: The Disease and Its Risk Factors OSTEOARTHRITIS: THE DISEASE AND ITS PREVALENCE AND IMPACT,» 2000.
- [5] E. Gardner, «Physiology of movable joints,» *Physiological Reviews*, vol. 30, n. 2, pp. 127-176, 1950.
- [6] N. Arden e M. C. Nevitt, «Osteoarthritis: Epidemiology,» *Best Practice and Research: Clinical Rheumatology*, vol. 20, n. 1, pp. 3-25, 2006.
- [7] F. Berenbaum, «Osteoarthritis as an inflammatory disease (osteoarthritis is not osteoarthrosis!),» *Osteoarthritis and Cartilage*, vol. 21, n. 1, pp. 16-21, 2013.
- [8] M. J. Benito, D. J. Veale, O. FitzGerald, W. B. Van Den Berg e B. Bresnihan, «Synovial tissue inflammation in early and late osteoarthritis,» *Annals of the Rheumatic Diseases*, vol. 64, n. 9, pp. 1263-1267, 9 2005.
- [9] F. Iannone e G. Lapadula, «The pathophysiology of osteoarthritis,» *Aging clinical and experimental research*, vol. 15, n. 5, pp. 364-372, 2003.
- [10] M. Kapoor, J. Martel-Pelletier, D. Lajeunesse, J. P. Pelletier e H. Fahmi, *Role of proinflammatory cytokines in the pathophysiology of osteoarthritis*, vol. 7, 2011, pp. 33-42.
- [11] A. J. Barr e P. G. Conaghan, «Disease-modifying osteoarthritis drugs (DMOADs): what are they and what can we expect from them,» *Medicographia*, vol. 35, pp. 189-196, 2013.
- [12] M. A. Karsdal, M. Michaelis, C. Ladel, A. S. Siebuhr, A. R. Bihlet, J. R. Andersen, H. Guehring, C. Christiansen, A. C. Bay-Jensen e V. B. Kraus, «Disease-modifying treatments for osteoarthritis (DMOADs) of the knee and hip: lessons learned from failures and opportunities for the future,» *Osteoarthritis and Cartilage*, vol. 24, n. 12, pp. 2013-2021, 2016.

- [13] P. Krinninger, R. Ensenauer, K. Ehlers, K. Rauh, J. Stoll, S. Krauss-Etschmann, H. Hauner e H. Laumen, «Peripheral monocytes of obese women display increased chemokine receptor expression and migration capacity,» *Journal of Clinical Endocrinology and Metabolism*, vol. 99, n. 7, pp. 2500-2509, 2014.
- [14] W. A. Muller, «How endothelial cells regulate transmigration of leukocytes in the inflammatory response,» *American Journal of Pathology*, vol. 184, n. 4, pp. 886-896, 2014.
- [15] W. A. Muller, «Leukocyte-endothelial-cell interactions in leukocyte transmigration and the inflammatory response,» *Trends in Immunology*, vol. 24, n. 6, pp. 326-333, 2003.
- [16] S. Nourshargh e R. Alon, «Leukocyte Migration into Inflamed Tissues,» *Immunity*, vol. 41, n. 5, pp. 694-707, 2014.
- [17] A. R. Schenkel, Z. Mamdouh e W. A. Muller, «Locomotion of monocytes on endothelium is a critical step during extravasation,» *Nature Immunology*, vol. 5, n. 4, pp. 393-400, 4 2004.
- [18] A. Urzainqui, J. M. Serrador, F. Viedma, M. Yáñez-Mó, A. Rodríguez, A. L. Corbí, J. L. Alonso-Lebrero, A. Luque, M. Deckert, J. Vázquez e F. Sánchez-Madrid, «ITAM-based interaction of ERM proteins with Syk mediates signaling by the leukocyte adhesion receptor PSGL-1,» *Immunity*, vol. 17, n. 4, pp. 401-412, 2002.
- [19] K. Ley, C. Laudanna, M. I. Cybulsky e S. Nourshargh, *Getting to the site of inflammation: The leukocyte adhesion cascade updated*, vol. 7, 2007, pp. 678-689.
- [20] J. Middleton, S. Neil, J. Wintle, I. Clark-Lewis, H. Moore, L. Charles, M. Auer, H. Elin e R. Antal, «Transcytosis and surface presentation of IL-8 by venular endothelial cells,» *Cell*, vol. 91, n. 3, pp. 385-395, 1997.
- [21] A. M. Bhosale e J. B. Richardson, *Articular cartilage: Structure, injuries and review of management*, vol. 87, 2008, pp. 77-95.
- [22] J. A. Buckwalter, H. J. Mankin e A. J. Grodzinsky, «Articular cartilage and osteoarthritis,» *Instructional Course Lectures-American Academy of Orthopaedic Surgeons*, vol. 54, p. 465, 2005.
- [23] A. J. Sophia Fox, A. Bedi e S. A. Rodeo, «The basic science of articular cartilage: Structure, composition, and function,» *Sports Health*, vol. 1, n. 6, pp. 461-468, 11 2009.
- [24] J. R. Ralphs e M. Benjamin, «The joint capsule: structure, composition, ageing and disease*,» 1994.
- [25] C. T. Vangsness, W. S. Burke, S. Narvy e A. N. Fedenko, «Human knee synovial fluid cytokines correlated with grade of knee osteoarthritis: A pilot study,» *Bulletin of the NYU hospital for joint diseases*, vol. 3, n. 111-125, 6.

- [26] T. M. Tamer, *Hyaluronan and synovial joint: Function, distribution and healing*, vol. 6, 2013, pp. 111-125.
- [27] E. Balazs, «The physical properties of synovial fluid and the special role of hyaluronic acid,» *Disorders of the Knee*, pp. 61-74, 1974.
- [28] P. Tabeling, *Introduction to microfluidics*, OUP Oxford, 2005.
- [29] A. Manz, N. Graber e H. M. Widmer, «Miniaturized Total Chemical Analysis Systems: a Novel Concept for Chemical Sensing,» 1990.
- [30] T. M. Squires e S. R. Quake, «Microfluidics: Fluid physics at the nanoliter scale,» *Reviews of modern physics*, vol. 77, n. 3, p. 977, 2005.
- [31] P. J. Kenis, R. F. Ismagilov e G. M. Whitesides, «Microfabrication inside capillaries using multiphase laminar flow patterning,» *Science*, vol. 285, n. 5424, pp. 83-85, 27 1999.
- [32] D. B. Weibel e G. M. Whitesides, «Applications of microfluidics in chemical biology,» *Current Opinion in Chemical Biology*, vol. 10, n. 6, pp. 584-591, 2006.
- [33] J. Pihl, M. Karlsson e D. T. Chiu, «Microfluidic technologies in drug discovery,» *Drug Discovery Today*, vol. 10, n. 20, pp. 1377-1383, 2005.
- [34] S. D. Minteer, *Microfluidic techniques: reviews and protocols (Vol. 321)*, Springer Science & Business Media, 2006.
- [35] Y. Xia e G. M. Whitesides, «Soft lithography,» *Annual review of materials science*, vol. 28, n. 1, pp. 153-184, 1998.
- [36] G. M. Whitesides, E. Ostuni, S. Takayama, X. Jiang e D. E. Ingber, «Soft Lithography in Biology and Biochemistry,» *Annual review of biomedical engineering*, vol. 3, n. 1, pp. 335-373, 2001.
- [37] J. C. McDonald e G. M. Whitesides, «Poly(dimethylsiloxane) as a material for fabricating microfluidic devices,» *Accounts of Chemical Research*, vol. 35, n. 7, pp. 491-499, 2002.
- [38] E. Delamarche, A. Bernard, H. Schmid, A. Bietsch, B. Michel e H. Biebuyck, «Microfluidic Networks for Chemical Patterning of Substrates: Design and Application to Bioassays,» *Journal of the American Chemical Society*, vol. 120, n. 3, pp. 500-508, 1998.
- [39] E. Berthier, E. W. Young e D. Beebe, *Engineers are from PDMS-land, biologists are from polystyrenia*, vol. 12, Royal Society of Chemistry, 2012, pp. 1224-1237.
- [40] M. Mehling e S. Tay, «Microfluidic cell culture,» *Current Opinion in Biotechnology*, vol. 25, pp. 95-102, 2014.

- [41] S. M. Ong, C. Zhang, Y. C. Toh, S. H. Kim, H. L. Foo, C. H. Tan, D. van Noort, S. Park e H. Yu, «A gel-free 3D microfluidic cell culture system,» *Biomaterials*, vol. 29, n. 22, pp. 3237-3244, 2008.
- [42] S. N. Bhatia e D. E. Ingber, *Microfluidic organs-on-chips*, vol. 32, Nature Publishing Group, 2014, pp. 760-772.
- [43] S. Piluso, Y. Li, F. Abinzano, R. Levato, L. Moreira Teixeira, M. Karperien, J. Leijten, R. van Weeren e J. Malda, «Mimicking the Articular Joint with In Vitro Models,» *Trends in Biotechnology*, 2019.
- [44] Y.-Y. Lin, N. Tanaka, S. Ohkuma, Y. Iwabuchi, Y. Tanne, T. Kamiya, R. Kunitatsu, Y.-C. Huang, M. Yoshioka, T. Mitsuyoshi, K. Tanimoto, E. Tanaka e K. Tanne, «Applying an excessive mechanical stress alters the effect of subchondral osteoblasts on chondrocytes in a co-culture system,» *European journal of oral sciences*, vol. 118, n. 2, pp. 151-158, 2010.
- [45] M. Beekhuizen, Y. M. Bastiaansen-Jenniskens, W. Koevoet, D. B. Saris, W. J. Dhert, L. B. Creemers e G. J. Van Osch, «Osteoarthritic synovial tissue inhibition of proteoglycan production in human osteoarthritic knee cartilage: Establishment and characterization of a long-term cartilage-synovium coculture,» *Arthritis and Rheumatism*, vol. 63, n. 7, pp. 1918-1927, 7 2011.
- [46] P. Occhetta, A. Mainardi, E. Votta, Q. Vallmajo-Martin, M. Ehrbar, I. Martin, A. Barbero e M. Rasponi, «Hyperphysiological compression of articular cartilage induces an osteoarthritic phenotype in a cartilage-on-a-chip model,» *Nature Biomedical Engineering*, vol. 3, n. 7, pp. 545-557, 1 7 2019.
- [47] H.-C. Chen, «Boyden Chamber Assay,» *Methods in Molecular Biology*, vol. 294, pp. 15-22, 2005.
- [48] T. M. Keenan e A. Folch, *Biomolecular gradients in cell culture systems*, vol. 8, Royal Society of Chemistry, 2007, pp. 34-57.
- [49] E. Bianchi, R. Molteni, R. Pardi e G. Dubini, «Microfluidics for in vitro biomimetic shear stress-dependent leukocyte adhesion assays,» *Journal of Biomechanics*, 2013.
- [50] J. Kitayama, A. Hidemura, H. Saito e H. Nagawa, «Shear stress affects migration behavior of polymorphonuclear cells arrested on endothelium,» *Cellular Immunology*, vol. 203, n. 1, pp. 39-46, 2000.
- [51] S. Han, J. J. Yan, Y. Shin, J. J. Jeon, J. Won, H. E. Jeong, R. D. Kamm, Y. J. Kim e S. Chung, «A versatile assay for monitoring in vivo-like transendothelial migration of neutrophils,» *Lab on a chip*, vol. 12, n. 20, pp. 3861-3865, 2012.
- [52] J. S. Jeon, S. Bersini, M. Gilardi, G. Dubini, J. L. Charest, M. Moretti e R. D. Kamm, «Human 3D vascularized organotypic microfluidic assays to study breast cancer cell extravasation,» *Proceedings of the National Academy of Sciences of the United States of America*, vol. 112, n. 1, pp. 214-219, 6 1 2015.

- [53] R. Molteni, E. Bianchi, P. Patete, M. Fabbri, G. Baroni, G. Dubini e R. Pardi, «A novel device to concurrently assess leukocyte extravasation and interstitial migration within a defined 3D environment,» *Lab on a Chip*, vol. 15, n. 1, pp. 195-207, 7 1 2015.
- [54] O. M. Klibanov, S. H. Williams e C. A. Iler, «Cenicriviroc, an orally active CCR5 antagonist for the potential treatment of HIV infection,» *Current Opinion in Investigational Drugs*, vol. 11, n. 8, pp. 940-950, 2010.
- [55] M. D. Dibonaventura, S. Gupta, M. McDonald e A. Sadosky, «Evaluating the health and economic impact of osteoarthritis pain in the workforce: Results from the National Health and Wellness Survey,» *BMC Musculoskeletal Disorders*, vol. 12, n. 1, p. 83, 2011.
- [56] J. Sellam e F. Berenbaum, *The role of synovitis in pathophysiology and clinical symptoms of osteoarthritis*, vol. 6, 2010, pp. 625-635.
- [57] A. E. I. Proudfoot, C. A. Power e M. K. Schwarz, «Anti-chemokine small molecule drugs: a promising future?,» *Expert Opinion on Investigational Drugs*, vol. 19, n. 3, pp. 345-355, 1 3 2010.
- [58] K. K. McDonald, S. Cooper, L. Danielzak e R. L. Leask, «Glycocalyx Degradation Induces a Proinflammatory Phenotype and Increased Leukocyte Adhesion in Cultured Endothelial Cells under Flow,» *PLOS ONE*, vol. 11, n. 12, pp. e0167576-, 1 12 2016.
- [59] A. Ohtsuka, J. Ando, R. Korenaga, A. Kamiya, N. Toyamasorimachi e M. Miyasaka, «The Effect of Flow on the Expression of Vascular Adhesion Molecule-1 by Cultured Mouse Endothelial Cells,» *Biochemical and Biophysical Research Communications*, vol. 193, n. 1, pp. 303-310, 1993.
- [60] M. Rahmati, A. Mobasheri e M. Mozafari, «Inflammatory mediators in osteoarthritis: A critical review of the state-of-the-art, current prospects, and future challenges,» *Bone*, vol. 85, pp. 81-90, 2016.
- [61] R. Oberoi, J. Schuett, H. Schuett, A.-K. Koch, M. Luchtefeld, K. Grote e B. Schieffer, «Targeting Tumor Necrosis Factor- α with Adalimumab: Effects on Endothelial Activation and Monocyte Adhesion,» *PLOS ONE*, vol. 11, n. 7, pp. e0160145-, 28 7 2016.
- [62] C. Jeng-Jiann, L. Pei-Ling, C. Cheng-Nan, L. Chih-I, C. Shun-Fu, C. Li-Jing, L. Sheng-Chieh, K. Ya-Chen, U. Shunichi e C. Shu, «Shear Stress Increases ICAM-1 and Decreases VCAM-1 and E-selectin Expressions Induced by Tumor Necrosis Factor- α in Endothelial Cells,» *Arteriosclerosis, Thrombosis, and Vascular Biology*, vol. 24, n. 1, pp. 73-79, 1 1 2004.
- [63] C. R. Scanzello, «Chemokines and inflammation in osteoarthritis: Insights from patients and animal models,» *Journal of Orthopaedic Research*, vol. 35, n. 4, pp. 735-739, 1 4 2017.
- [64] M. B. Goldring e M. Otero, «Inflammation in osteoarthritis,» *Current opinion in rheumatology*, vol. 23, n. 5, pp. 471-478, 9 2011.

- [65] K. Gaspar, G. Kukova, E. Bunemann, B. A. Buhren, E. Sonkoly, A. G. Szollosi, A. Muller, T. Savinko, A. I. Lauerma, H. Alenius, L. Kemeny, M.-C. Dieu-Nosjean, S. Stander, J. W. Fischer, T. Ruzicka, A. Zlotnik, A. Szegedi e B. Homey, «The chemokine receptor CCR3 participates in tissue remodeling during atopic skin inflammation,» *Journal of Dermatological Science*, vol. 71, n. 1, pp. 12-21, 2013.
- [66] M. Baba, K. Takashima, H. Miyake, N. Kanzaki, K. Teshima, X. Wang, M. Shiraishi e Y. Iizawa, «TAK-652 Inhibits CCR5-Mediated Human Immunodeficiency Virus Type 1 Infection In Vitro and Has Favorable Pharmacokinetics in Humans,» *Antimicrobial Agents and Chemotherapy*, vol. 49, n. 11, p. 4584, 11 2005.
- [67] H. Yang, M. Bocchetta, B. Kroczyńska, A. G. Elmishad, Y. Chen, Z. Liu, C. Bubici, B. T. Mossman, H. I. Pass, J. R. Testa, G. Franzoso e M. Carbone, «TNF- α inhibits asbestos-induced cytotoxicity via a NF- κ B-dependent pathway, a possible mechanism for asbestos-induced oncogenesis,» *Proceedings of the National Academy of Sciences*, vol. 103, n. 27, p. 10397, 5 7 2006.